1. The initial state $\boldsymbol{s}_1$ is chosen following the initial probability $p(\boldsymbol{s})$.
2. For $t = 1, \ldots, T$,
   (a) The action a_t is chosen following the policy $\pi(a_t|\boldsymbol{s}_t)$.
   (b) The next state $\boldsymbol{s}_{t+1}$ is determined according to the transition probability $p(\boldsymbol{s}_{t+1}|\boldsymbol{s}_t, a_t)$.

FIGURE 1.11: Generation of a trajectory sample.

When the number of steps, T, is finite or infinite, the situation is called the *finite horizon* or *infinite horizon*, respectively. Below, we focus on the finite-horizon case because the trajectory length is always finite in practice. We denote a trajectory by h (which stands for a "*history*"):

$$h = [\boldsymbol{s}_1, a_1, \ldots, \boldsymbol{s}_T, a_T, \boldsymbol{s}_{T+1}].$$

The discounted sum of immediate rewards along the trajectory h is called the *return*:

$$R(h) = \sum_{t=1}^{T} \gamma^{t-1} r(\boldsymbol{s}_t, a_t, \boldsymbol{s}_{t+1}),$$

where $\gamma \in [0, 1)$ is called the *discount factor* for future rewards.

The goal of reinforcement learning is to learn the optimal policy π^* that maximizes the *expected return*:

$$\pi^* = \underset{\pi}{\operatorname{argmax}}\, \mathbb{E}_{p^\pi(h)}\Big[R(h)\Big],$$

where $\mathbb{E}_{p^\pi(h)}$ denotes the expectation over trajectory h drawn from $p^\pi(h)$, and $p^\pi(h)$ denotes the probability density of observing trajectory h under policy π:

$$p^\pi(h) = p(\boldsymbol{s}_1) \prod_{t=1}^{T} p(\boldsymbol{s}_{t+1}|\boldsymbol{s}_t, a_t)\pi(a_t|\boldsymbol{s}_t).$$

"argmax" gives the maximizer of a function (Figure 1.12).

For policy learning, various methods have been developed so far. These methods can be classified into *model-based reinforcement learning* and *model-free reinforcement learning*. The term "model" indicates a model of the transition probability $p(\boldsymbol{s}'|\boldsymbol{s}, a)$. In the model-based reinforcement learning approach, the transition probability is learned in advance and the learned transition model is explicitly used for policy learning. On the other hand, in the model-free reinforcement learning approach, policies are learned without explicitly estimating the transition probability. If strong prior knowledge of the

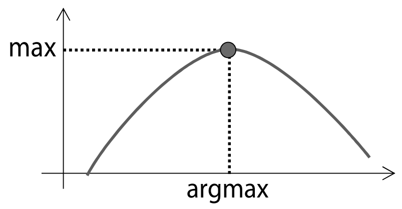

FIGURE 1.12: "argmax" gives the maximizer of a function, while "max" gives the maximum value of a function.

transition model is available, the model-based approach would be more favorable. On the other hand, learning the transition model without prior knowledge itself is a hard statistical estimation problem. Thus, if good prior knowledge of the transition model is not available, the model-free approach would be more promising.

1.3 Structure of the Book

In this section, we explain the structure of this book, which covers major reinforcement learning approaches.

1.3.1 Model-Free Policy Iteration

Policy iteration is a popular and well-studied approach to reinforcement learning. The key idea of policy iteration is to determine policies based on the *value function*.

Let us first introduce the *state-action value function* $Q^\pi(\boldsymbol{s}, a) \in \mathbb{R}$ for policy π, which is defined as the expected return the agent will receive when taking action a at state $\boldsymbol{s}$ and following policy π thereafter:

$$Q^\pi(\boldsymbol{s}, a) = \mathbb{E}_{p^\pi(h)}\left[R(h)\middle|\boldsymbol{s}_1 = \boldsymbol{s}, a_1 = a\right],$$

where "$|\boldsymbol{s}_1 = \boldsymbol{s}, a_1 = a$" means that the initial state $\boldsymbol{s}_1$ and the first action a_1 are fixed at $\boldsymbol{s}_1 = \boldsymbol{s}$ and $a_1 = a$, respectively. That is, the right-hand side of the above equation denotes the conditional expectation of $R(h)$ given $\boldsymbol{s}_1 = \boldsymbol{s}$ and $a_1 = a$.

Let $Q^*(\boldsymbol{s}, a)$ be the optimal state-action value at state $\boldsymbol{s}$ for action a defined as

$$Q^*(\boldsymbol{s}, a) = \max_\pi Q^\pi(\boldsymbol{s}, a).$$

Based on the optimal state-action value function, the optimal action the agent should take at state $\boldsymbol{s}$ is deterministically given as the maximizer of $Q^*(\boldsymbol{s}, a)$

1. Initialize policy $\pi(a|\boldsymbol{s})$.
2. Repeat the following two steps until the policy $\pi(a|\boldsymbol{s})$ converges.
   (a) Policy evaluation: Compute the state-action value function $Q^\pi(\boldsymbol{s}, a)$ for the current policy $\pi(a|\boldsymbol{s})$.
   (b) Policy improvement: Update the policy as
   $$\pi(a|\boldsymbol{s}) \longleftarrow \delta\left(a - \underset{a'}{\operatorname{argmax}}\, Q^\pi(\boldsymbol{s}, a')\right).$$

FIGURE 1.13: Algorithm of policy iteration.

with respect to a. Thus, the optimal policy $\pi^*(a|\boldsymbol{s})$ is given by

$$\pi^*(a|\boldsymbol{s}) = \delta\left(a - \underset{a'}{\operatorname{argmax}}\, Q^*(\boldsymbol{s}, a')\right),$$

where $\delta(\cdot)$ denotes Dirac's delta function.

Because the optimal state-action value Q^* is unknown in practice, the policy iteration algorithm alternately evaluates the value Q^π for the current policy π and updates the policy π based on the current value Q^π (Figure 1.13).

The performance of the above policy iteration algorithm depends on the quality of policy evaluation; i.e., how to learn the state-action value function from data is the key issue. Value function approximation corresponds to a *regression* problem in statistics and machine learning. Thus, various statistical machine learning techniques can be utilized for better value function approximation. Part II of this book addresses this issue, including least-squares estimation and model selection (Chapter 2), basis function design (Chapter 3), efficient sample reuse (Chapter 4), active learning (Chapter 5), and robust learning (Chapter 6).

1.3.2 Model-Free Policy Search

One of the potential weaknesses of policy iteration is that policies are learned via value functions. Thus, improving the quality of value function approximation does not necessarily contribute to improving the quality of resulting policies. Furthermore, a small change in value functions can cause a big difference in policies, which is problematic in, e.g., robot control because such instability can damage the robot's physical system. Another weakness of policy iteration is that policy improvement, i.e., finding the maximizer of $Q^\pi(\boldsymbol{s}, a)$ with respect to a, is computationally expensive or difficult when the action space $\mathcal{A}$ is continuous.

Policy search, which directly learns policy functions without estimating value functions, can overcome the above limitations. The basic idea of policy search is to find the policy that maximizes the expected return:

$$\pi^* = \underset{\pi}{\operatorname{argmax}}\, \mathbb{E}_{p^\pi(h)}\Big[R(h)\Big].$$

In policy search, how to find a good policy function in a vast function space is the key issue to be addressed. Part III of this book focuses on policy search and introduces gradient-based methods and the expectation-maximization method in Chapter 7 and Chapter 8, respectively. However, a potential weakness of these direct policy search methods is their instability due to the stochasticity of policies. To overcome the instability problem, an alternative approach called *policy-prior search*, which learns the policy-prior distribution for deterministic policies, is introduced in Chapter 9. Efficient sample reuse in policy-prior search is also discussed there.

1.3.3 Model-Based Reinforcement Learning

In the above model-free approaches, policies are learned without explicitly modeling the unknown environment (i.e., the transition probability of the agent in the environment, $p(\boldsymbol{s}'|\boldsymbol{s}, a)$). On the other hand, the model-based approach explicitly learns the environment in advance and uses the learned environment model for policy learning.

No additional sampling cost is necessary to generate artificial samples from the learned environment model. Thus, the model-based approach is particularly useful when data collection is expensive (e.g., robot control). However, accurately estimating the transition model from a limited amount of trajectory data in multi-dimensional continuous state and action spaces is highly challenging. Part IV of this book focuses on model-based reinforcement learning. In Chapter 10, a non-parametric transition model estimator that possesses the optimal convergence rate with high computational efficiency is introduced. However, even with the optimal convergence rate, estimating the transition model in high-dimensional state and action spaces is still challenging. In Chapter 11, a *dimensionality reduction* method that can be efficiently embedded into the transition model estimation procedure is introduced and its usefulness is demonstrated through experiments.

CHAPTER 5

DEEP LEARNING FOR FEATURE REPRESENTATION

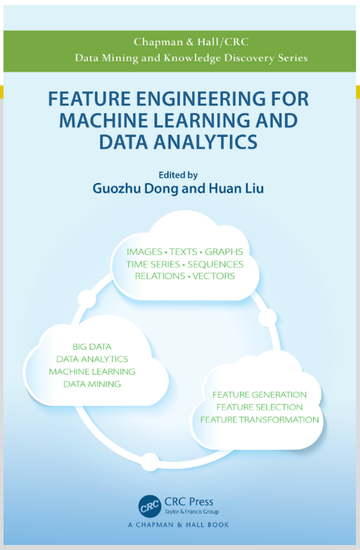
Chapman & Hall/CRC Data Mining and Knowledge Discovery Series

FEATURE ENGINEERING FOR MACHINE LEARNING AND DATA ANALYTICS

Edited by Guozhu Dong and Huan Liu

Deep Learning for Feature Representation

Suhang Wang

Arizona State University

Huan Liu

Arizona State University

11.1 Introduction

Deep learning methods have become increasingly popular in recent years because of their tremendous success in image classification [19], speech recognition [20] and natural language processing tasks [60]. In fact, deep learning methods have regularly won many recent challenges in these domains [19]. The great success of deep learning mainly comes from specially designed structures of deep nets, which are able to learn discriminative non-linear features that can facilitate the task at hand. For example, the specially designed convolutional layers of CNN allow it to extract translation-invariant features from images while the max pooling layers of CNN help to reduce the parameters to be learned. In essence, the majority of existing deep learning algorithms can be used as powerful feature learning/extraction tools, i.e., the *latent features* extracted by deep learning algorithms are the new learned representations. In this chapter, we will review classical and popular deep learning algorithms and explain how they can be used for feature representation learning. We will also discuss how they are used for hierarchical and disentangled representation learning, and how they can be applied to various domains.

11.2 Restricted Boltzmann Machine

A restricted Boltzmann machine (RBM) is an undirected graphical model that defines a probability distribution over a vector of observed, or visible, variables $\mathbf{v} \in \{0,1\}^m$ and a vector of latent, or hidden, variables $\mathbf{h} \in \{0,1\}^d$, where m is the dimension of input features and d is the dimension of the latent features. It is widely used for unsupervised representation learning. For example, $\mathbf{v}$ can be the bag-of-words representation of documents or the vectorized binary images and $\mathbf{h}$ *is the learned representation for the input data.* A typical choice is that $d < m$, i.e., learning compact representation. Figure 11.1(a) gives a toy example of an RBM. In the figure, each node of the hidden layer is connected to each node in the visible layer, while there are no connections between hidden nodes or visible nodes. Figure 11.1(b) is a simplified representation of RBM, where the connection details between hidden layers and visible layers are simplified. We will begin by assuming both $\mathbf{v}$ and $\mathbf{h}$ as binary vectors, i.e., elements of $\mathbf{v}$ and $\mathbf{h}$ can only take the value of 0 or 1. An extension of real-valued input $\mathbf{x}$ will be introduced 11.2.2. An RBM defines a joint probability over $\mathbf{v}$ and $\mathbf{h}$ as

$$P(\mathbf{v},\mathbf{h}) = \frac{1}{Z}\exp(-E(\mathbf{v},\mathbf{h})) \tag{11.1}$$

where Z is the partition function defined as $Z = \sum_{\mathbf{v}}\sum_{\mathbf{h}}\exp(-E(\mathbf{v},\mathbf{h}))$, and E is an energy function given by

$$E(\mathbf{v},\mathbf{h}) = -\mathbf{h}^T\mathbf{W}\mathbf{v} - \mathbf{b}^T\mathbf{h} - \mathbf{c}^T\mathbf{v} \tag{11.2}$$

where $\mathbf{W} \in \mathbb{R}^{d\times m}$ is a matrix of pairwise weights between elements of $\mathbf{v}$ and $\mathbf{h}$ (see Figure 11.1(a)), while $\mathbf{b} \in \mathbb{R}^{d\times 1}$ and $\mathbf{c} \in \mathbb{R}^{m\times 1}$ are biases for the hidden and visible variables, respectively.[1]

[1]For simplicity, bias terms are not shown in Figure 11.1.

Since there are no explicit connections between hidden units in an RBM, given randomly selected training data $\mathbf{v}$, the hidden units are independent of each other, which gives $P(\mathbf{h}|\mathbf{v}) = \prod_{i=1}^{d} P(h_i|\mathbf{v})$, and the binary state, h_i, $i = 1, \ldots, d$, is set to 1 with conditional probability given as,

$$P(h_i = 1|\mathbf{v}) = \sigma\big(\sum_{j=1}^{m} W_{ij} v_j + b_i\big) \tag{11.3}$$

where $\sigma(\cdot)$ is the sigmoid function defined as $\sigma(x) = (1 + \exp(-x))^{-1}$. Similarly, given $\mathbf{h}$, the visible units are independent of each other. Thus, we have $P(\mathbf{v}|\mathbf{h}) = \prod_{j=1}^{m} P(v_j|\mathbf{h})$, and the binary state, v_j, $j = 1, \ldots, m$, is set to 1 with conditional probability given as

$$P(v_j = 1|\mathbf{h}) = \sigma(\sum_{i=1}^{d} W_{ij} h_i + v_j). \tag{11.4}$$

With the simple conditional probabilities given by Eq.(11.3) and Eq.(11.4), sampling from $P(\mathbf{h}|\mathbf{v})$ and $P(\mathbf{v}|\mathbf{h})$ becomes very efficient. RBMs have generally been trained using gradient ascent to maximize the log-likelihood $l(\boldsymbol{\theta})$ for some set of training vectors $\mathbf{V} \in \mathbb{R}^{m \times n}$, where $\boldsymbol{\theta} = \{\mathbf{W}, \mathbf{b}, \mathbf{c}\}$ is the set of variables to be optimized. The log-likelihood $l(\boldsymbol{\theta})$ is written as

$$l(\boldsymbol{\theta}) = \frac{1}{n} \log P(\mathbf{V}) = \frac{1}{n} \sum_{i=1}^{n} \log P(\mathbf{v}_i). \tag{11.5}$$

The derivative of $\log P(\mathbf{v})$ w.r.t variable $\mathbf{W}$ is given as

$$\frac{\partial \log P(\mathbf{v})}{\partial \mathbf{W}} = \sum_{\mathbf{h}} P(\mathbf{h}|\mathbf{v}) \mathbf{h} \mathbf{v}^T - \sum_{\tilde{\mathbf{v}}} \sum_{\mathbf{h}} P(\tilde{\mathbf{v}}, \mathbf{h}) \mathbf{h} \tilde{\mathbf{v}}^T \tag{11.6}$$

where $\tilde{\mathbf{v}} \in \{0,1\}^m$ is an m-dimensional binary vector. The first term in Eq.(11.6) can be computed exactly. This term is often referred to as the *positive* gradient. It corresponds to the expected gradient of the energy with respect to $P(\mathbf{h}|\mathbf{v})$. The second term in Eq. (11.6) is known as the *negative* gradient, which is expectation over the model distribution $P(\mathbf{v}, \mathbf{h})$. It is intractable to compute the negative gradients exactly. Thus, we need to approximate the negative gradients by sampling $\mathbf{v}$ from $P(\mathbf{v}|\mathbf{h})$ and sampling $\mathbf{h}$ from $P(\mathbf{h}|\mathbf{v})$ by maintaining a Gibbs chain. For more details, we encourage readers to refere to Contrastive Divergence [62].

11.2.1 Deep Belief Networks and Deep Boltzmann Machine

RBMs can be stacked and trained in a greedy manner to form so-called Deep Belief Networks (DBN) [21] . DBNs are graphical models which learn

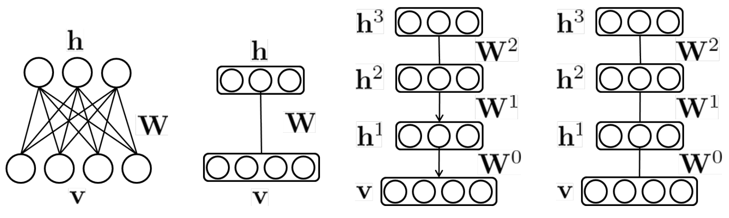

(a) RBM (b) RBM (c) 3-layer DBN (d) 3-layer DBM

Figure 11.1: An illustration of RBM, DBN and DBM.

to extract a deep hierarchical representation of the training data. They model the joint distribution between observed vector $\mathbf{v}$ and the l hidden layers as:

$$P(\mathbf{x}, \mathbf{h}^1, \mathbf{h}^2, \ldots, \mathbf{h}^l) = \left(\prod_{k=0}^{l-2} P(\mathbf{h^k} | \mathbf{h^{k+1}}) \right) P(\mathbf{h}^{l-1}, \mathbf{h}^l) \tag{11.7}$$

where $\mathbf{v} = \mathbf{h}^0$. $P(\mathbf{h}^{k-1} | \mathbf{h}^k)$ is a conditional distribution for the visible units conditioned on the hidden units of the RBM at level k, and $P(\mathbf{h}^{l-1}, \mathbf{h}^l)$ is the visible-hidden joint distribution in the top-level RBM. This is illustrated in Figure 11.1(c). DBN is able to learn hierarchical representation [33]. The low-level hidden representation such as $\mathbf{h}^1$ captures *low-level features* while the high-level hidden representation such as $\mathbf{h}^3$ captures more complex *high-level features.* Training of DBN is done by greedy layer-wise unsupervised training [21]. Specifically, we first train the first layer as an RBM with the raw input $\mathbf{v}$. From the first layer, we obtain the latent representation as the mean activations $P(\mathbf{h}^1|\mathbf{h}^0)$ or samples of $P(\mathbf{h}^1|\mathbf{h}^0)$, which will then be used as input to the second layer to update $\mathbf{W}^2$. After all the layers are trained, we can fine-tune all the parameters of DBN with respect to a proxy for the DBN log-likelihood, or with respect to a supervised training criterion by adding a classifier such as the softmax function on top of DBN.

A deep Boltzmann machine (DBM) [51] is another kind of deep generative model. Figure 11.1(d) gives an illustration of a DBM with 3 hidden layers. Unlike DBN, it is an entirely undirected model. Unlike RBM, the DBM has several layers of latent variables (RBMs have just one). Within each layer, each of the variables are mutually independent, conditioned on the variables in the neighboring layers. In the case of a deep Boltzmann machine with one visible layer $\mathbf{v}$, and l hidden layers, $\mathbf{h}^1$, $\mathbf{h}^2$ and $\mathbf{h}^l$, the joint probability is given by:

$$P(\mathbf{v}, \mathbf{h}^1, \mathbf{h}^2, \ldots, \mathbf{h}^n) = \frac{1}{Z} \exp(-E(\mathbf{v}, \mathbf{h}^1, \mathbf{h}^2, \ldots, \mathbf{h}^n)) \tag{11.8}$$

where the DBM energy function is defined as

$$E(\mathbf{v}, \mathbf{h}^1, \mathbf{h}^2, \ldots, \mathbf{h}^n) = -(\sum_{k=0}^{l-1} \mathbf{h}^k \mathbf{W}^k \mathbf{h}^{k+1}) - \sum_k \mathbf{b}^k \mathbf{h}^k \tag{11.9}$$

and $\mathbf{v} = \mathbf{h}^0$, $\mathbf{W}^k$ is the weight matrix to capture the interaction between $\mathbf{h}^k$ and $\mathbf{h}^{k+1}$, and $\mathbf{b}^k$ is the bias.

The conditional distribution over one DBM layer given the neighboring layers is factorial. In the example of the DBM with two hidden layers, these distributions are $P(\mathbf{v}|\mathbf{h}^1)$, $P(\mathbf{h}^1|\mathbf{v}, \mathbf{h}^2)$ and $P(\mathbf{h}^2|\mathbf{h}^1)$. The distribution over all hidden layers generally does not factorize because of interactions between layers. In the example with two hidden layers, $P(\mathbf{h}^1, \mathbf{h}^2|\mathbf{v})$ does not factorize due to the interaction weights $\mathbf{W}^1$ between $\mathbf{h}^1$ and $\mathbf{h}^2$ which render these variables mutually dependent. Therefore, sampling from $P(\mathbf{h}^1, \mathbf{h}^2|\mathbf{v})$ is difficult while training of DBM using gradient ascent methods require sampling from $P(\mathbf{h}^1, \mathbf{h}^2|\mathbf{v})$. To solve this problem, we use a mean-field approximation to approximate $P(\mathbf{h}^1, \mathbf{h}^2|\mathbf{v})$. Specifically, we define

$$Q(\mathbf{h}^1, \mathbf{h}^2) = \prod_j Q(h_j^1|\mathbf{v}) \prod_k Q(h_k^2|\mathbf{v}) \tag{11.10}$$

The mean field approximation attempts to find a member of this family of distributions that best fits the true posterior $P(\mathbf{h}^1, \mathbf{h}^2|\mathbf{v})$ by minimizing KL-divergence between $Q(\mathbf{h}^1, \mathbf{h}^2)$ and $P(\mathbf{h}^1, \mathbf{h}^2|\mathbf{v})$. With the approximation, we can easily sample $\mathbf{h}^1$ and $\mathbf{h}^2$ from $Q(\mathbf{h}^1, \mathbf{h}^2)$ and then update the parameters using gradient ascents with these samples [51].

11.2.2 RBM for Real-Valued Data

In many real-world applications such as image and audio modeling, the input features $\mathbf{v}$ are often real-valued data. Thus, it is important to extend RBM for modeling real-valued inputs. There are many variants of the RBM which defines the probability over real-valued data such as Gaussian-Bernoulli RBMs [69], mean and variance RBMs [22] and Spike and Slab RBMs [8].

The Gaussian-Bernoulli RBM (GBM) is the most common way to handle real-valued data, which has binary hidden units and real-valued visible units. It assumes the conditional distribution over the visible units being a Gaussian distribution whose mean is a function of the hidden units. Under this assumption, GRBM defines a joint probability over $\mathbf{v}$ and $\mathbf{h}$ as in Eq.(11.1) with the energy function given as

$$E(\mathbf{v}, \mathbf{h}) = -\mathbf{h}^T\mathbf{W}(\mathbf{v} \odot \boldsymbol{\beta}) - \mathbf{b}^T\mathbf{h} - \frac{1}{2}\mathbf{v} - \mathbf{c}^T(\boldsymbol{\beta} \odot (\mathbf{v} - \mathbf{c})) \tag{11.11}$$

where $\boldsymbol{\beta} \in \mathbb{R}^{m\times 1}$ is the precision vector with the i-th element β_i being the precision of v_i. $\odot$ is the Hadamard operation. Then the conditional probability of $P(\mathbf{v}|\mathbf{h})$ and $P(\mathbf{h}|\mathbf{v})$ are

$$P(\mathbf{h}|\mathbf{v}) = \prod_{i=1}^{d} P(h_i|\mathbf{v}) = \prod_{i=1}^{d} \sigma(b_i + \sum_{j=1}^{m} W_{ij} v_i \beta_i) \tag{11.12}$$

$$P(\mathbf{v}|\mathbf{h}) = \prod_{j=1}^{m} P(v_j|\mathbf{h}) = \prod_{j=1}^{m} \mathcal{N}(v_j|b_j + \sum_{i=1}^{d} W_{ij}h_i, \beta_i^{-1}) \tag{11.13}$$

where $\mathcal{N}(v_j|b_j + \sum_{i=1}^{d} W_{ij}h_i, \beta_i^{-1})$ is the Gaussian distribution with mean $b_j + \sum_{i=1}^{d} W_{ij}h_i$ and variance β_i^{-1}.

While the GRBM has been the canonical energy model for real-valued data, it is not well suited to the statistical variations present in some types of real-valued data, especially natural images [31]. The problem is that much of the information content present in natural images is embedded in the covariance between pixels rather than in the raw pixel values. To solve these problems, alternative models have been proposed that attempt to better account for the covariance of real-valued data. Mean and Covariance RBM (mcRBM) is one of the alternatives. The mcRBM uses its hidden units to independently encode the conditional mean and covariance of all observed units. Specifically, the hidden layer of mcRBM is divided into two groups of units: binary mean units $\mathbf{h}^{(m)}$ and binary covariance units $\mathbf{h}^{(c)}$. The energy function of mcRBM is defined as the combination of two energy functions:

$$E_{mc}(\mathbf{v}, \mathbf{h}^{(m)}, \mathbf{h}^{(c)}) = E_m(\mathbf{v}, \mathbf{h}^{(m)}) + E_c(\mathbf{v}, \mathbf{h}^{(c)}) \tag{11.14}$$

where $E_m(\mathbf{v}, \mathbf{h}^{(m)})$ is the standard Gaussian-Bernoulli energy function defined in Eq.(11.11), which models the interaction between real-valued $\mathbf{v}$ input and hidden units $\mathbf{h}^{(m)}$; and $E_c(\mathbf{v}, \mathbf{h}^{(c)})$ models the conditional covariance information, which is given as

$$E_c(\mathbf{v}, \mathbf{h}^{(c)}) = \frac{1}{2}\sum_j h_j^{(c)}(\mathbf{v}^T\mathbf{r}^{(j)})^2 - \sum_j b_j^{(c)}h_j^{(c)}. \tag{11.15}$$

The parameter $\mathbf{r}^{(j)}$ corresponds to the covariance weight vector associated with $h_j^{(c)}$ and $\mathbf{b}^{(c)}$ is a vector of covariance offsets.

11.3 AutoEncoder

An autoencoder (AE) is a neural network trained to learn latent representation that is good at reconstructing its input [4]. Generally, an autoencoder is composed of two parts, i.e., an encoder $f(\cdot)$ and a decoder $g(\cdot)$. An illustration of autoencoder is shown in Figure 11.2(a). The encoder maps the input $\mathbf{x} \in \mathbb{R}^m$ to latent representation $\mathbf{h} \in \mathbb{R}^d$ as $\mathbf{h} = f(\mathbf{x})$ and $f(\cdot)$ is usually a one-layer neural network, i.e., $f(\mathbf{x}) = s(\mathbf{W}\mathbf{x} + \mathbf{b})$, where $\mathbf{W} \in \mathbb{R}^{d\times m}$ and $\mathbf{b} \in \mathbb{R}^d$ are the weights and bias of the encoder. $s(\cdot)$ is a non-linear function such as sigmoid and tanh. A decoder maps back the latent representation $\mathbf{h}$ into a reconstruction $\tilde{\mathbf{x}} \in \mathbb{R}^m$ as $\tilde{\mathbf{x}} = g(\mathbf{h})$ and $g(\cdot)$ is given as $g(\mathbf{h}) = s(\mathbf{W}'\mathbf{h} + \mathbf{b}')$, where $\mathbf{W}^{'} \in \mathbb{R}^{m\times d}$ and $\mathbf{b} \in \mathbb{R}^{m}$ are the weights and bias of the decoder. Note that the prime symbol does not indicate matrix transposition. The parameters of the autoencoder, i.e., $\theta = \{\mathbf{W}, \mathbf{b}, \mathbf{W}', \mathbf{b}'\}$ are optimized to minimize the reconstruction error. Depending on the appropriate distribution assumptions of the input, the reconstruction error can be measured in many ways. The most widely used reconstruction error is the squared error $\mathcal{L}(\mathbf{x}, \tilde{\mathbf{x}}) = \|\mathbf{x} - \tilde{\mathbf{x}}\|_2^2$. Alternatively, if the input is interpreted as either bit vectors or vectors of bit probabilities, cross-entropy of the reconstruction can be used

$$\mathcal{L}_H(\mathbf{x}, \tilde{\mathbf{x}}) = -\sum_{k=1}^{d}[\mathbf{x}_k \log \tilde{\mathbf{x}}_k + (1 - \mathbf{x}_k \log(1 - \tilde{\mathbf{x}}_k))]. \tag{11.16}$$

By training an autoencoder that is good at reconstructing input data, we hope that the latent representation $\mathbf{h}$ can capture some useful features. The identity function seems a particularly trivial function to try to learn, when it doesn't result in useful features. Therefore, we need to add constraints to the autoencoder to avoid trivial solution and learn useful features.

The autoencoder can be used to extract useful features by forcing $\mathbf{h}$ to have smaller dimension than $\mathbf{x}$, i.e., $d < m$. An autoencoder whose latent dimension is less than the input dimension is called an undercomplete autoencoder. Learning an undercomplete representation forces the autoencoder to capture the most salient features of the training data [15]. In other words, the latent representation $\mathbf{h}$ is a distributed representation which captures the coordinates along the main factors of variation in the data [15]. This is similar to the way that the projection on principal components would capture the main factors of variation in the data. Indeed, if there is one linear hidden layer, i.e., no activation function applied, and the mean squared error criterion is used to train the network, then the d hidden units learn to project the input in the span of the first d principal components of the data. If the hidden layer is non-linear, the autoencoder behaves differently from PCA, with the ability to capture multi-modal aspects of the input distribution.

Another choice is to constrain $\mathbf{h}$ to have a larger dimension than $\mathbf{x}$, i.e., $d > m$. An autoencoder whose latent dimension is larger than the input dimension is called an overcomplete autoencoder. However, due to the large dimension, the encoder and decoder are given too much capacity. In such cases, even a linear encoder and linear decoder can learn to copy the input to the output without learning anything useful about the data distribution. Fortunately, we can still discover interesting structure, by imposing other constraints on the network. One of the most widely used constraints is the sparsity constraint on $\mathbf{h}$. An overcomplete autoencoder with sparsity constraint is called a sparse autoencoder, which will be discussed next.

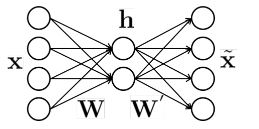

(a) Autoencoder

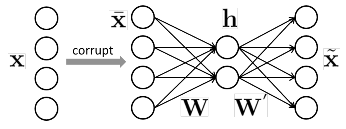

(b) Denoising AE

Figure 11.2: An illustration of an autoencoder and a denoising autoencoder.

11.3.1 Sparse Autoencoder

A sparse autoencoder is an overcomplete authoencorder which tries to learn sparse overcomplete codes that are good at reconstruction [43]. A sparse overcomplete representation can be viewed as an alternative "compressed" representation: it has implicit straightforward compressibility due to the large number of zeros rather than an explicit lower dimensionality. Given the training data $\mathbf{X} \in \mathbb{R}^{m \times N}$, the objective function is given as

$$\min_{\mathbf{W},\mathbf{b},\mathbf{W}',\mathbf{b}'} \frac{1}{N} \sum_{i=1}^{N} \mathcal{L}(\mathbf{x}_i, \tilde{\mathbf{x}}_i) + \alpha\Omega(\mathbf{h}_i) \tag{11.17}$$

where N is the number of training instances, $\mathbf{x}_i$ is the i-th training instance, and $\mathbf{h}_i$ and $\tilde{\mathbf{x}}_i$ are the corresponding latent representation and reconstructed features. $\Omega(\mathbf{h}_i)$ is the sparsity regularizer to make $\mathbf{h}_i$ sparse and α is a scalar to control the sparsity. Many sparsity regularizers can be adopted. One popularly used is the ℓ_1-norm, i.e., $\Omega(\mathbf{h}_i) = \|\mathbf{h}_i\|_1 = \sum_{j=1}^{d} |h_i(j)|$. However, the ℓ_1-norm is non-smooth and not appropriate for gradient descent. An alternative is to use the smooth sparse constraint based on KL-divergence. Let ρ_j, $j = 1, \dots, d$ be the average activation of hidden unit j (averaged over the training set) as

$$\rho_j = \frac{1}{N} \sum_{i=1}^{N} \mathbf{h}_i(j). \tag{11.18}$$

The essential idea is to force ρ_j to be close to ρ, where ρ is a small value close to zero (say $\rho = 0.05$). By forcing ρ_j be close to ρ, we would like the average activation of each hidden neuron j to be close to 0.05 (say). This constraint is satisfied when the hidden unit activations are mostly near 0. To achieve that ρ_j is close to ρ, we can use the KL-divergence as

$$\sum_{j=1}^{d} KL(\rho||\rho_j) = \sum_{j=1}^{d} \rho \log \frac{\rho}{\rho_j} + (1-\rho) \log \frac{1-\rho}{1-\rho_j}. \tag{11.19}$$

$KL(\rho||\rho_j)$ is a convex function with its minimum of when $\rho_j = \rho$. Thus, minimizing this penalty term has the effect of causing ρ_j to be close to ρ, which achieves the sparse effect.

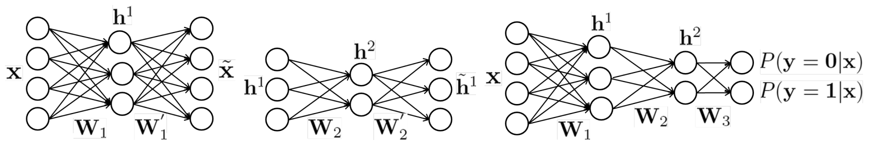

(a) 1st Autoencoder (b) 2nd Autoencoder (c) Fine-tuning

Figure 11.3: An illustration of 2-layer stacked autoencoder.

11.3.2 Denoising Autoencoder

The aforementioned autoencoders add constraints on latent representations to learn useful features. Alternatively, denoising the autoencoder uses the denoising criteria to learn useful features. In order to force the hidden layer to discover more robust features and prevent it from simply learning the identity, the denoising autoencoder trains the autoencoder to reconstruct the input from a corrupted version of it [63]. An illustration of denoising autoencoder is shown in Figure 11.2(b). In the figure, the clean data $\mathbf{x}$ is first corrupted as a noisy data $\bar{\mathbf{x}}$ by means of a stochastic mapping $q_D(\bar{\mathbf{x}}|\mathbf{x})$. The corrupted data $\bar{\mathbf{x}}$ is then used as input to an autoencoder, which outputs the reconstructed data $\tilde{\mathbf{x}}$. The training objective of a denoising autoencoder is then to make reconstructed data $\tilde{\mathbf{x}}$ close to the clean data $\mathbf{x}$ as $\mathcal{L}(\mathbf{x}, \tilde{\mathbf{x}})$.

There are many choices of the stochastic mapping such as (1) additive isotropic Gaussian noise (GS): $\bar{\mathbf{x}}|\mathbf{x} \sim N(\mathbf{x}, \sigma\mathbf{I})$; this is a very common noise model suitable for real-valued inputs. (2) Masking noise (MN): a fraction ν of the elements of x (chosen at random for each example) is forced to 0. (3) Salt-and-pepper noise (SP): a fraction ν of the elements of $\mathbf{x}$ (chosen at random for each example) is set to their minimum or maximum possible value (typically 0 or 1) according to a fair coin flip. The masking noise and salt-and-pepper noise are natural choices for input domains which are interpretable as binary or near binary such as black-and-white images or the representations produced at the hidden layer after a sigmoid squashing function [63].

11.3.3 Stacked Autoencoder

Denoising autoencoders can be stacked to form a deep network by feeding the latent representation of the DAE found on the layer below as input to the current layer as shown in Figure 11.3, which are generally called stacked denoising autoencoders (SDAEs). The unsupervised pre-training of such an architecture is done one layer at a time. Each layer is trained as a DAE by minimizing the error in reconstructing its input. For example, in Figure 11.3(a), we train the first layer autoencoder. Once the first layer is trained, we can train the 2nd layer with the latent representation of the first autoencoder, i.e., $\mathbf{h}^1$, as input. This is shown in Figure 11.3(b). Once all layers are pre-trained, the network goes through a second stage of training called fine-tuning, which is typically to minimize prediction error on a supervised task. For fine-tuning, we first add a logistic regression layer on top of the network as shown in Figure 11.3(c) (more precisely on the output code of the output layer). We then train the entire network as we would train a multilayer perceptron. At this point, we only consider the encoding parts of each autoencoder. This stage is supervised, since now we use the target class during training.

11.4 Convolutional Neural Networks

The Convolutional Neural Network (CNN or ConvNet) has achieved great success in many computer vision tasks such as image classification [32], segmentation [36] and video action recognition [55]. The specially designed architecture of the CNN is very powerful in extracting visual features from images, which can be used for various tasks. An example of a simplified CNN is shown in Figure 11.4. It is comprised of three basic types of layers, which are convolutional layers for extracting translation-invariant features from images, pooling layers for reducing the parameters and fully connected layers for classification tasks. CNNs are mainly formed by stacking these layers together. Recently, dropout layers [56] and residual layers [19] are also introduced to prevent CNN from overfitting and to ease the training of deep CNNs, respectively. Next, we will introduce the basic building blocks of CNNs and how CNNs can be used for feature learning.

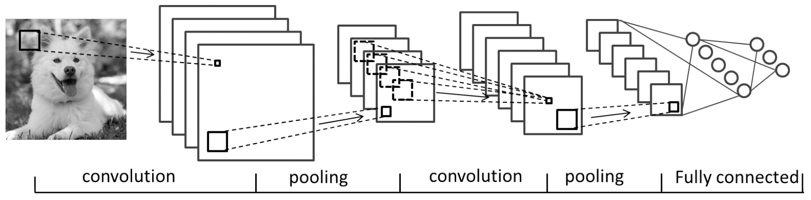

Figure 11.4: An illustration of CNN.

The Convolutional Layer: As the name implies, the Conv layer is the core building block of a CNN. The essential idea of a Conv layer is the observation that natural images have the property of being "stationary," which means that the statistics of one part of the image are the same as any other part. For example, a dog can appear in any location of an image. This suggests that the dog feature detector that we learn at one part of the image can also be applied to other parts of the image to detect dogs, and we can use the same features at all locations. More precisely, having learned features over small (say 3x3) patches sampled randomly from the larger image, we can then apply this learned 3x3 feature detector anywhere in the image. Specifically, we can take the learned 3x3 features and "convolve" them with the larger image, thus obtaining a different feature activation value at each location in the image. The feature detector is called a filter or kernel in ConvNet and the feature obtained is called a feature map. Figure 11.5 gives an example of a convolution operation with the input as the 5x5 matrix and the kernel as the 3x3 matrix. The 3x3 kernel slides over the 5x5 matrix from left to right and from the top to down, which generates the feature map shown on the right. The convolution is done by multiplying the kernel by the sub-patch of the input feature map and then sum together. For example, the calculation of the gray sub-patch in the 5x5 matrix with the kernel is given in the figure. There

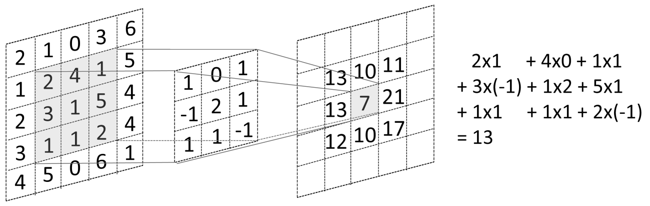

Figure 11.5: An illustration of convolution operation.

are three parameters in a Conv layer, i.e., the *depth*, *stride* and *zero-padding. Depth* corresponds to the number of filters we would like to use. A Conv layer can have many filters, each learning to look for something different in the input. For example, if the first Conv layer takes as input the raw image, then different neurons along the depth dimension may activate in the presence of various oriented edges, or blobs of color. In the simple ConvNet shown in Figure 11.4, the depth of the first convolution and second convolution layers are 4 and 6, respectively. *Stride* specifies how many pixels we skip when we slide the filter over the input feature map. When the stride is 1, we move the filters one pixel at a time as shown in Figure 11.5. When the stride is 2, the filters jump 2 pixels at a time as we slide them around. This will produce smaller output volumes spatially. It will be convenient to pad the input volume with zeros around the border, which is called *zero-padding.* The size of this zero-padding is a hyperparameter. The nice feature of zero-padding is that it will allow us to control the spatial size of the output volumes. Let the input volume be $W \times H \times K$, where W and H are width and height of the feature map and K is the number of feature maps. For example, for a color image with RGB channels, we have $K = 3$. Let the receptive field size (filter size) of the Conv Layer be F, number of filters be $\tilde{K}$, the stride with which they are applied be S, and the amount of zero padding used on the border be P; then the output volume after convolution is $\tilde{W} \times \tilde{H} \times \tilde{K}$, where $\tilde{W} = (W - F + 2P)/S + 1$ and $\tilde{H} = (H - F + 2P)/S + 1$. For example, for a $7 \times 7 \times 3$ input and a $4 \times 3 \times 3$ filter with stride 1 and pad 0, we would get a $5 \times 5 \times 4$ output.

Convolution using filters is a linear operation. After the feature maps are obtained in a Conv layer, a nonlinear activation function will be applied on these feature maps to learn non-linear features. Rectified linear unit (ReLU) is the most widely used activation function for ConvNet, which is demonstrated

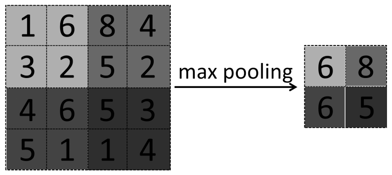

Figure 11.6: An illustration of a max pooling operation.

to be effective in alleviating the gradient vanishing problem. A rectifier is defined as $f(x) = \max(0, x)$.

The Pooling Layer: Pooling layers are usually periodically inserted between successive Conv layers in a CNN. They aim to progressively reduce the spatial size of the representation, which can help reduce the number of parameters and computation in the network, and hence also control overfitting. The pooling layer operates independently over each activation map in the input, and scales its dimensionality using the *max* function. The most common form is a pooling layer with filters of size 2x2 applied with a stride of 2, which downsamples every depth slice in the input by 2 along both width and height, discarding 75% of the activations. Every max operation would, in this case, be taking a max over 4 numbers and the maximum value of the 4 numbers will go to the next layer. An example of a max pooling operation is shown in Figure 11.6. During the forward pass of a pooling layer it is common to keep track of the index of the max activation (sometimes also called the switches) so that gradient routing is efficient during backpropagation.

Though max pooling is the most popular pooling layer, a CNN can also contain general pooling. General pooling layers are comprised of pooling neurons that are able to perform a multitude of common operations including L1/L2-normalization, and average pooling. An example of max pooling

The Fully Connected Layer: Neurons in a fully connected layer have full connections to all activations in the previous layer, as shown in Figure 11.4. The fully connected layers are put at the end of a CNN architecture, i.e., after several layers of Conv layer and max pooling layers. With the high-level features extracted by the previous layers, fully connected layers will then attempt to produce class scores from the activations, to be used for classification. The output of the fully connected layer will then be put in a softmax for classification. It is also suggested that ReLu may be used as the activation function in a fully connected layer to improve performance.

11.4.1 Transfer Feature Learning of CNN

In practice, training an entire Convolutional Network from scratch (with random initialization) is rare as (1) it is very time consuming and requires many computation resources and (2) it is relatively rare to have a dataset of sufficient size to train a ConvNet. Therefore, instead, it is common to pre-train a ConvNet on a very large dataset (e.g., ImageNet, which contains 1.2 million images with 1000 categories), and then use the ConvNet either as an initialization or a fixed feature extractor for the task of interest [53]. There are mainly two major Transfer Learning scenarios, which are listed as follows:

- ConvNet as a fixed feature extractor: In this scenario, we take a ConvNet pretrained on ImageNet, remove the last fully connected layer, then treat the rest of the ConvNet as a fixed feature extractor for the new dataset. With the extracted features, we can train a linear classifier such as Linear SVM or logistic regression for the new dataset. This is usually used when the new dataset is small and similar to the original dataset. For such datasets, training or fine-tuning a ConvNet is not practical as ConvNets are prone to overfitting to small datasets. Since the new dataset is similar to the original dataset, we can expect higher-level features in the ConvNet to be relevant to this dataset as well.

- Fine-tuning the ConvNet: The second way is to not only replace and retrain the classifier on top of the ConvNet on the new dataset, but to also fine-tune the weights of the pretrained network using backpropagation. The essential idea of fine-tuning is that the earlier features of a ConvNet contain more generic features (e.g., edge detectors or color blob detectors) that should be useful in many tasks, but later layers of the ConvNet become progressively more specific to the details of the classes contained in the original dataset. If the new dataset is large enough, we can fine-tune all the layers of the ConvNet. If the new dataset is small but different from the original dataset, then we can keep some of the earlier layers fixed (due to overfitting concerns) and only fine-tune some higher-level portion of the network.

11.5 Word Embedding and Recurrent Neural Networks

Word embedding and recurrent neural networks are the state-of-the-art deep learning models for natural language processing tasks. Word embedding learns word representation and recurrent neural networks utilize word embedding for sentence or document feature learning. Next, we introduce the details of word embedding and recurrent neural networks.

11.5.1 Word Embedding

Word embedding, or distributed representation of words, is to represents each word as a low-dimensional dense vector such that the vector representation of words can capture synthetic and semantic meanings of words. The low-dimensional representation can also alleviate the curse of dimensionality and data sparsity problems suffered by traditional representations such as bag-of-words and N-gram [66]. The essential idea of word embedding is the distributional hypothesis that "you shall know a word by the company it keeps" [13]. This suggests that a word has close relationships with its neighboring words. For example, the phrases *win the game* and *win the lottery* appear very frequently; thus the pair of words *win* and *game* and the pair of words *win* and *lottery* could have a very close relationship. When we are only given the word *win*, we would highly expect the neighboring words to be words like *game* or *lottery* instead of words as *light* or *air*. This suggests that a good word representation should be useful for predicting its neighboring words, which is the essential idea of Skip-gram [41]. In other words, the training objective of the Skip-gram model is to find word representations that are useful for predicting the surrounding words in a sentence or a document. More formally, given a sequence of training words $w_1, w_2, \ldots, w_T$, the objective of the Skip-gram model is to maximize the average log probability

$$\frac{1}{T}\sum_{t=1}^{T}\sum_{-c\leq j\leq c, j\neq 0}\log P(w_{t+j}|w_t) \tag{11.20}$$

where c is the size of the training context (which can be a function of the center word w_t). Larger c results in more training examples and thus can lead to higher accuracy, at the expense of training time. The basic Skip-gram formulation defines $P(w_{t+j}|w_t)$ using the softmax function:

$$P(w_O|w_I) = \frac{\exp(\mathbf{u}_{w_O}^T \mathbf{v}_{w_I})}{\sum_{w=1}^{W}\exp(\mathbf{u}_w{}^T \mathbf{v}_{w_I})} \tag{11.21}$$

where $\mathbf{v}_w$ and $\mathbf{u}_w$ are the "input" and "output" representations of w, and W is the number of words in the vocabulary. Learning the representation is usually done by gradient descent. However, Eq.(11.21) is impractical because the cost of computing $\nabla \log P(w_O|w_I)$ is proportional to W, which is often large. One way of making the computation more tractable is to replace the softmax in Eq. (11.21) with a hierarchical softmax. In a hierarchical softmax, the vocabulary is represented as a Huffman binary tree with words as leaves. With the Huffman tree, the probability of $P(w_O|w_I)$ is the probability of walking the path from root node to leaf node w_O given the word w_I, which is calculated as decision making in each node along the path with a simple function. Huffman trees assign short binary codes to frequent words, and this further reduces the number of output units that need to be evaluated. Another alternative to make the computation tractable is negative sampling [41]. The essential idea of negative sampling is that w_t should be more similar to its neighboring words, say w_{t+j}, than randomly sampled words. Thus, the objective function of negative sampling is to maximize the similarity between w_t and w_{t+j} and minimize the similarity between w_t and randomly sampled words. With negative sampling, Eq. (11.21) is approximated as

$$\log \sigma(\mathbf{u}_{W_O}^T \mathbf{v}_{w_I}) + \frac{1}{K}\sum_{i=1}^{K} \log \sigma(-\mathbf{u}_{W_i}^T \mathbf{v}_{w_I}) \tag{11.22}$$

where K is the number of negative words sampled for each input word w_I. It is found that skip-gram with negative sampling is equivalent to implicitly factorizing a word-context matrix, whose cells are the pointwise mutual information (PMI) of the respective word and context pairs, shifted by a global constant [34].

Instead of using the center words to predict the context (surrounding words in a sentence), Continuous Bag-of-Words Model (CBOW) predicts the current word based on the context. More precisely, CBOW uses each current word as an input to a log-linear classifier with a continuous projection layer, and predicts words within a certain range before and after the current word [39]. The objective function of CBOW is to maximize the following log-likelihood function

$$\frac{1}{T}\sum_{t=1}^{T} \log P(w_t | w_{t-c}, \ldots, w_{t-1}, w_{t+1}, \ldots, w_{t+c}) \tag{11.23}$$

and $P(w_t | w_{t-c}, \ldots, w_{t-1}, w_{t+1}, \ldots, w_{t+c})$ is defined as

$$P(w_t | w_{t-c}, \ldots, w_{t-1}, w_{t+1}, \ldots, w_{t+c}) = \frac{\exp(\mathbf{u}_{w_t}{}^T \tilde{\mathbf{v}}_t)}{\sum_{w=1}^{W} \exp(\mathbf{u}_{w}{}^T \tilde{\mathbf{v}}_t)} \tag{11.24}$$

where $\tilde{\mathbf{v}}_t$ is the average representation of the contexts of w_t, i.e., $\tilde{\mathbf{v}}_t = \frac{1}{2c}\sum_{-c \le j \le c, j \ne 0} \mathbf{v}_{t+j}$.

Methods like skip-gram may do better on the analogy task, but they poorly utilize the statistics of the corpus since they train on separate local context windows instead of on global co-occurrence counts. Based on this observation, GloVe, proposed in [46], uses a specific weighted least squares model that trains on global word-word co-occurrence counts and thus makes efficient use of statistics. The objective function of GloVe is given as

$$\min \sum_{i,j} f(X_{ij})(\mathbf{w}_i^T \tilde{\mathbf{w}}_j - \log X_{ij})^2 \tag{11.25}$$

where X_{ij} tabulates the number of times word j occurs in the context of word i. $\mathbf{w}_i \in \mathbb{R}^d$ is the word representation of w_i and $\tilde{\mathbf{w}}_j$ is a separate context word vector. $f()$ is the weighting function.

Word embedding can capture syntactic and semantic meanings of words. For example, it is found that vec(queen) is the closest vector representation to vec(king) - vec(man) + vec(woman), which implies that word representation learned by Skip-gram encodes semantic meanings of words. Word embedding can also be used for document representation by averaging the word vectors of words appearing in a document as the vector representation of the documents.

Following the distributional representation idea of word embedding, many network embedding algorithms are proposed. The essential idea of network embedding is to learn vector representations of network nodes that are good at predicting the neighboring nodes.

Since word representation learned by word embedding algorithms are low-dimensional dense vectors that capture semantic meanings, they are widely used as a preprocessing step in deep learning methods such as recurrent neural networks and recursive neural networks. Each word will be mapped to a vector representation before it is used as input to deep learning models.

11.5.2 Recurrent Neural Networks

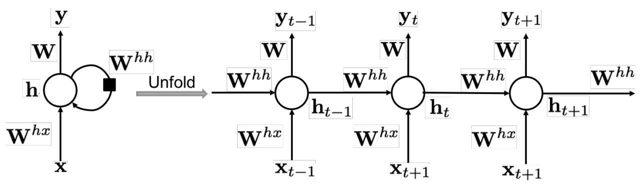

Figure 11.7: An illustration of an RNN.

Recurrent neural networks (RNN) are powerful concepts that allow the use of loops within the neural network architecture to model sequential data such as sentences and videos. Recurrent networks take as input a sequence of inputs, and produce a sequence of outputs. Thus, such models are particularly useful for sequence-to-sequence learning.

Figure 11.7 gives an illustration of the RNN architecture. The left part of the figure shows a folded RNN, which has a self-loop, i.e., the hidden state $\mathbf{h}$ is used to update itself given an input $\mathbf{x}$. To better show how RNN works, we unfold the RNN as a sequential structure, which is given in the right part of Figure 11.7. The RNN takes a sequence, $\mathbf{x}_1, \mathbf{x}_2, \dots, \mathbf{x}_t, \dots, \mathbf{x}_T$ as input, where at each step t, $\mathbf{x}_t$ is a d-dimensional feature vector. For example, if the input is a sentence, then each word w_i of the sentence is represented as a vector $\mathbf{x}_i$ using word embedding methods such as Skip-gram. At each time-step t, the output of the previous step, $\mathbf{h}_{t-1}$, along with the next word vector in the document, $\mathbf{x}_t$, are used to update the hidden state $\mathbf{h}_t$ as

$$\mathbf{h}_t = \sigma(\mathbf{W}^{hh}\mathbf{h}_{t-1} + \mathbf{W}^{hx}\mathbf{x}_t) \tag{11.26}$$

where $\mathbf{W}^{hh} \in \mathbb{R}^{d\times d}$ and $\mathbf{W}^{hx} \in \mathbb{R}^{d\times d}$ are the weights for inputs $\mathbf{h}_{t-1}$ and $\mathbf{x}_t$, respectively. *The hidden states $\mathbf{h}_t$ is the feature representation of the sequence up to time t for the input sequence.* The initial states $\mathbf{h}_0$ are usually initialized as all 0. Thus, we can utilize $\mathbf{h}_t$ to perform various tasks such as sentence completion and document classification. For example, for a sentence completion task, we are given the partial sentence, "The weather is..." and

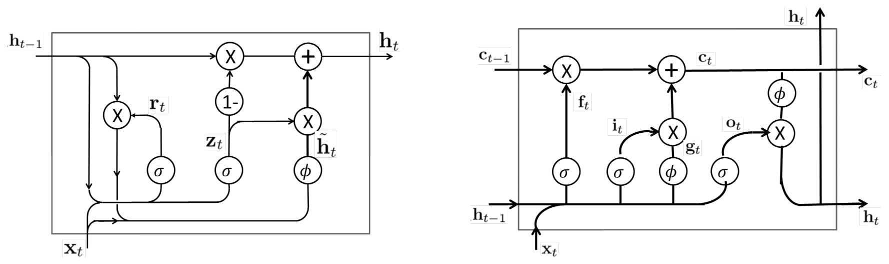

(a) One GRU Cell (b) One LSTM Cell

Figure 11.8: An illustration of GRU and LSTM cells.

we want to predict the next word. We can predict the next word as

$$\mathbf{y}_t = softmax(\mathbf{W}\mathbf{h}_t + \mathbf{b}), \quad y_t = \arg\max \mathbf{y}_t \tag{11.27}$$

where $\mathbf{W} \in \mathbb{R}^{V \times d}$ are the weights of the softmax function with V being the size of the vocabulary and b the bias term. $\mathbf{y}_t$ is the predicted probability vector and y_t is the predicted label. We can think of an RNN as modeling the likelihood probability as $P(\mathbf{y}_t|\mathbf{x}_1, \ldots, \mathbf{x}_t)$.

Training of RNNs is usually done using Backpropagation Through Time (BPTT), which back propagates the error from time t to time 1 [70].

11.5.3 Gated Recurrent Unit

Though in theory, RNN is able to capture long-term dependency, in practice, the old memory will fade away as the sequence becomes longer. To make it easier for RNNs to capture long-term dependencies, gated recurrent units (GRUs) [7] are designed to have more persistent memory. Unlike an RNN, which uses a simple affine transformation of $\mathbf{h}_{t-1}$ and $\mathbf{h}_t$ followed by *tanh* to update $\mathbf{h}_t$, GRU introduces the Reset Gate to determine if it wants to forget past memory and the Update Gate to control if new inputs are introduced to $\mathbf{h}_t$. The mathematical equations of how this is achieved are given as follows and an illustration of a GRU cell is shown in Figure 11.8(a):

$$\begin{aligned}
\mathbf{z}_t &= \sigma(\mathbf{W}_{zx}\mathbf{x}_t + \mathbf{W}_{zh}\mathbf{h}_{t-1} + \mathbf{b}_z) && \text{(Update gate)}\\
\mathbf{r}_t &= \sigma(\mathbf{W}_{rx}\mathbf{x}_t + \mathbf{W}_{rh}\mathbf{h}_{t-1} + \mathbf{b}_r) && \text{(Reset gate)}\\
\tilde{\mathbf{h}}_t &= \tanh(\mathbf{r}_t \odot \mathbf{U}\mathbf{h}_{t-1} + \mathbf{W}\mathbf{x}_t) && \text{(New memory)}\\
\mathbf{h}_t &= (1 - \mathbf{z}_t) \odot \tilde{\mathbf{h}}_t + \mathbf{z}_t \odot \mathbf{h}_{t-1} && \text{(Hidden state)}
\end{aligned} \tag{11.28}$$

From the above equation and Figure 11.8(a), we can treat the GRU as four fundamental operational stages, i.e., new memory, update gate, reset gate and hidden state. A new memory $\tilde{h}_t$ is the consolidation of a new input word $\mathbf{x}_t$ with the past hidden state $\mathbf{h}_{t-1}$, which summarizes this new word in light of the contextual past. The reset signal $\mathbf{r}_t$ is used to determining how important

$\mathbf{h}_{t-1}$ is to the summarization $\tilde{\mathbf{h}}_t$. The reset gate has the ability to completely diminish a past hidden state if it finds that $\mathbf{h}_{t-1}$ is irrelevant to the computation of the new memory. The update signal $\mathbf{z}_t$ is responsible for determining how much of past state $\mathbf{h}_{t-1}$ should be carried forward to the next state. For instance, if $\mathbf{z}_t \approx 1$, then $\mathbf{h}_{t-1}$ is almost entirely copied out to $\mathbf{h}_t$. The hidden state $\mathbf{h}_t$ is finally generated using the past hidden input $\mathbf{h}_t$ and the new memory generated $\tilde{\mathbf{h}}_t$ with the control of the update gate.

11.5.4 Long Short-Term Memory

Long Short-Term Memories, LSTMs [23], are another variant of the RNN, which can also capture long-term dependency. Similar to GRUs, an LSTM introduces more complex gates to control if it should accept new information or forget previous memory, i.e., the input gate, forget gate, output gate and new memory cell. The update rules of LSTMs are given as follows:

$$\begin{aligned}
\mathbf{i}_t &= \sigma(\mathbf{W}_{ix}\mathbf{x}_t + \mathbf{W}_{ih}\mathbf{h}_{t-1} + \mathbf{b}_i) && \text{(Input gate)}\\
\mathbf{f}_t &= \sigma(\mathbf{W}_{fx}\mathbf{x}_t + \mathbf{W}_{fh}\mathbf{h}_{t-1} + \mathbf{b}_f) && \text{(Forget gate)}\\
\mathbf{o}_t &= \sigma(\mathbf{W}_{ox}\mathbf{x}_t + \mathbf{W}_{oh}\mathbf{h}_{t-1} + \mathbf{b}_o) && \text{(Output gate)}\\
\mathbf{g}_t &= \tanh(\mathbf{W}_{gx}\mathbf{x}_t + \mathbf{W}_{gh}\mathbf{h}_{t-1} + \mathbf{b}_g) && \text{(New memory cell)}\\
\mathbf{c}_t &= \mathbf{f}_t \odot \mathbf{c}_{t-1} + \mathbf{i}_t \odot \mathbf{g}_t && \text{(Final memory cell)}\\
\mathbf{h}_t &= \mathbf{o}_t \odot \tanh(\mathbf{c}_t) && (11.29)
\end{aligned}$$

where $\mathbf{i}_t$ is the input gate, $\mathbf{f}_t$ is the forget gate, $\mathbf{o}_t$ is the forget fate, $\mathbf{c}_t$ is the memory cell state at t and $\mathbf{x}_t$ is the input features at t. $\sigma(\cdot)$ means the sigmoid function and $\odot$ denotes the Hadamard product. The main idea of the LSTM model is the memory cell $\mathbf{c}_t$, which records the history of the inputs observed up to t. $\mathbf{c}_t$ is a summation of (1) the previous memory cell $\mathbf{c}_{t-1}$ modulated by a sigmoid gate $\mathbf{f}_t$, and (2) $\mathbf{g}_t$, a function of previous hidden states and the current input modulated by another sigmoid gate $\mathbf{i}_t$. The sigmoid gate $\mathbf{f}_t$ is to selectively forget its previous memory while $\mathbf{i}_t$ is to selectively accept the current input. $\mathbf{i}_t$ is the gate controlling the output. The illustration of a cell of LSTM at the time step t is shown in Figure 11.8(b).

11.6 Generative Adversarial Networks and Variational Autoencoder

In this section, we introduce two very popular deep generative models proposed recently, i.e., generative adversarial networks and the variational autoencoder.

11.6.1 Generative Adversarial Networks

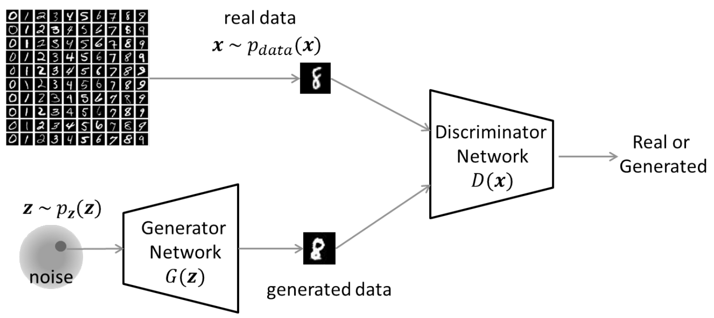

Figure 11.9: An illustration of the framework of the GAN.

The generative adversarial network (GAN) [16] is one of the most popular generative deep models. The core of a GAN is to play a min-max game between a discriminator D and a generator G, i.e., adversarial training. The discriminator D tries to differentiate if a sample is from the real world or generated by the generator, while the generator G tries to generate samples that can fool the discriminator, i.e., make the discriminator believe that the generated samples are from the real world. Figure 11.9 gives an illustration of the framework of the GAN. The generator takes a noise $\mathbf{z}$ sampled from a prior distribution $p_{\mathbf{z}}(\mathbf{z})$ as input, and maps the noise to the data space as $G(\mathbf{z}; \theta_g)$. Typical choices of the prior $p(\mathbf{z})$ can be a uniform distribution or Gaussian distribution. We also define a second multilayer perceptron $D(\mathbf{x}; \theta_d)$ that outputs a single scalar. $D(\mathbf{x})$ represents the probability that $\mathbf{x}$ came from the real-world data rather than generated data. D is trained to maximize the probability of assigning the correct label to both training examples and samples from G. We simultaneously train G to minimize $\log(1 - D(G(\mathbf{z})))$. In other words, D and G play the following two-player minimax game with value function $V(D, G)$:

$$\min_G \max_D V(D,G) = \mathbb{E}_{\mathbf{x}\sim p_{data}(\mathbf{x})}[\log D(\mathbf{x})] + \mathbb{E}_{\mathbf{z}\sim p_{\mathbf{z}(\mathbf{z})}}[\log(1 - D(G(\mathbf{z})))]. \tag{11.30}$$

The training of a GAN can be done using minibatch stochastic gradient descent training by updating the parameters of G and D alternatively. *After the model is trained without supervision, we can treat the discriminator as a feature extractor*: The first few layers of D extract features from $\mathbf{x}$ while the last few layers are to map the features to the probability that $\mathbf{x}$ is from real data. Thus, we can remove the last few layers, then the output of D is the features extracted. In this sense, we treat GANs as unsupervised feature learning algorithms, though the main purpose of the GAN is to learn $p(\mathbf{x})$.

The GAN is a general adversarial training framework, which can be used for various domains by designing a different generator, discriminator and loss function [6, 65, 74]. For example, InfoGAN [6] learns disentangled representation by dividing the noise into two parts, i.e., disentangled codes **c** and incompressible noise **z** so that the disentangled codes **c** can control the properties such as the identity and illumination of the images generated. SeqGAN [74] models the data generator as a stochastic policy in reinforcement learning and extends the GAN for text generation.

11.6.2 Variational Autoencoder

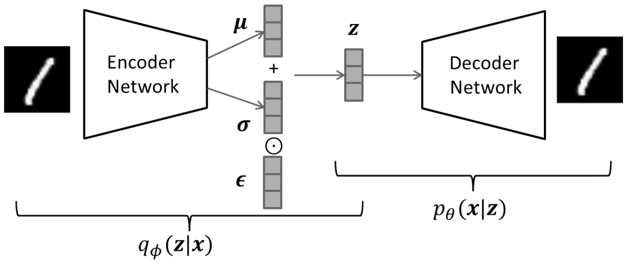

Figure 11.10: An illustration of the framework of the VAE.

The variational autoencoder (VAE) [30] is a popular generative model for unsupervised representation learning. It can be trained purely with gradient-based methods. Typically, a VAE has a standard autoencoder component which encodes the input data into a latent code space by minimizing reconstruction error, and a Bayesian regularization over the latent space, which forces the posterior of the hidden code vector to match a prior distribution. Figure 11.10 gives an illustration of a VAE. To generate a sample from the model, the VAE first draws a sample $\mathbf{z}$ from the prior distribution $p_\theta(\mathbf{z})$. The sample $\mathbf{z}$ is used as input to a differentiable generator network $g(\mathbf{z})$. Finally, $\mathbf{x}$ is sampled from a distribution $p_\theta(\mathbf{x}|g(\mathbf{z})) = p_\theta(\mathbf{x}|\mathbf{z})$. During the training, the approximate inference network, i.e., encoder network $q_\phi(\mathbf{z}|\mathbf{x})$, is then used to obtain $\mathbf{z}$ and $p_\theta(\mathbf{x}|\mathbf{z})$ is then viewed as a decoder network. The core idea of variational autoenoder is that they are trained by maximizing the variational lower bound $\mathcal{L}(\theta, \phi; \mathbf{x})$:

$$\mathcal{L}(\theta, \phi; \mathbf{x}) = -D_{KL}(q_\phi(\mathbf{z}|\mathbf{x})||p_\theta(\mathbf{z})) + \mathbb{E}_{q_\phi(\mathbf{z}|\mathbf{x})}[\log p_\theta(\mathbf{x}|\mathbf{z})] \leq \log p_\theta(\mathbf{x}) \tag{11.31}$$

where $D_{KL}(q_\phi(\mathbf{z}|\mathbf{x})||p_\theta(\mathbf{z}))$ is the KL divergence which measures the similarity of two distributions $q_\phi(\mathbf{z}|\mathbf{x})$ and $p_\theta(\mathbf{z})$. ϕ and θ are the variational parameters and generative parameters, respectively. We want to differentiate and optimize the lower bound w.r.t both the ϕ and θ. However, directly using a gradient estimator for the above objective function will exhibit high variance. Therefore, VAE adopts the reparametric trick. That is, under certain mild conditions for a chosen approximate posterior $q_\phi(\mathbf{z}|\mathbf{x})$, the random variable $\tilde{z} \sim q_\phi(\mathbf{z}|\mathbf{x})$ can be parameterized as

$$\tilde{z} = g_\phi(\epsilon, \mathbf{x}) \quad \text{with} \quad \epsilon \sim p(\epsilon) \tag{11.32}$$

where $g_\phi(\epsilon, \mathbf{x})$ is a differentiable transformation function of a noise variable ϵ. The nonparametric trick is also shown in Figure 11.10. With this technique, the variational lower bound in Eq.(11.31) can be approximated as

$$\begin{aligned} L^A(\theta, \phi; \mathbf{x}) &= \frac{1}{L}\sum_{l=1}^{L} \log p_\theta(\mathbf{x}, \mathbf{z}^{(l)}) - \log q_\phi(\mathbf{z}^{(l)}|\mathbf{x}) \\ \tilde{z}^{(l)} &= g_\phi(\epsilon^{(l)}, \mathbf{x}) \quad \text{with} \quad \epsilon^{(l)} \sim p(\epsilon). \end{aligned} \tag{11.33}$$

Then the parameters can be learned via stochastic gradient descent efficiently. It is easy to see that the encoder is a feature extractor which learns latent representations for $\mathbf{x}$.

11.7 Discussion and Further Readings

We have introduced representative deep learning models for feature engineering. In this section, we'll discuss how they can be used for hierarchical representation learning and disentangled representation, and how they can be used for popular domains such as text, image and graph.

Table 11.1: Hierarchical and disentangled representation learning

Method	Hierarchical Fea. Rep.	Disentangled Fea. Rep.
RBM/DBM	[59]	[48]
DBN	[33]	N/A
AE/DAE/SDAE	[37]	[28]
RNN/GRU/LSTM	[68,73]	[11,54]
CNN	[12,14]	[25,49]
GAN	[47]	[6,38]
VAE	[75]	[54,72]

Hierarchical Representation Generally, hierarchical representation lets us learn features of hierarchy and combine top-down and bottom-up processing of an image (or text). For instance, lower layers could support object detection by spotting low-level features indicative of object parts. Conversely, information about objects in the higher layers could resolve lower-level ambiguities in the image or infer the locations of hidden object parts. Features at different hierarchy levels may be good for different tasks. The high-level features captures the main objects, resolve ambiguities, and thus are good for classification, while mid-level features include many details and may be good for segmentation. Hierarchical feature representation is very common in deep learning models. We list some representative literature on how the introduced model can be used for hierarchical feature learning in Table 11.1.

Disentangled Representation Disentangled representation is a popular way to learn explainable representations. The majority of existing representation learning frameworks learn representation $\mathbf{h} \in \mathbb{R}^{d\times 1}$, which is difficult to explain, i.e., the d-latent dimensions are entangled together and we don't know the semantic meaning of the d-dimensions. Instead, disentangled representation learning tries to disentangle the latent factors so we know the semantic meaning of the latent dimensions. For example, for handwritten digits such as the MNIST dataset, we may want to disentangle the digit shape from writing style so that some part of $\mathbf{h}$ controls digit shapes while the other part represents writing style. The disentangled representation not only explains latent representation but also helps generate controlled realistic images. For example, by changing the part of codes that controls digit shape, we can generate new images of target digit shapes using a generator with this new latent representation. Therefore, disentangled representation learning is attracting increasing attention. Table 11.1 also lists some representative deep learning methods for disentangled representation learning. This is still a relatively new direction that needs further investigation.

Table 11.2: Deep learning methods for different domains

Method	Text	Image	Audio	Linked Data) (Graph)
RBM/DBM	[57,58]	[57]	[9]	[67]
DBN	[52]	[33]	[42]	N/A
AE/DAE/SDAE	[3]	[63]	[44]	[64]
CNN	[29]	[19,45,71]	[1]	[10]
Word2Vec	[35,41]	N/A	N/A	[61,66]
RNN/GRU/LSTM	[27,40,60]	[2]	[17,50]	N/A
GAN	[74]	[6,47]	[74]	N/A
VAE	[5,26]	[18,30]	[24]	N/A

Deep Feature Representation for Various Domains Many deep learning algorithms were initially developed for specific domains. For example, the CNN was initially developed for image processing and Word2Vec was initially proposed for learning word representation. Due to the great success of these methods, they were further developed to be applicable to other domains. For example, in addition to images, the CNN has also been successfully applied on texts, audio and linked data. Each domain has its own unique property. For example, text data are inherently sequential and graph data are non-i.i.d. Thus, directly applying CNN is impractical. New architectures are proposed to adapt the CNN for these domains. The same holds for the other deep learning algorithms. Therefore, we summarize the application of the discussed deep learning models in four domains in Table 11.2. We encourage interested users to read these papers for further understanding.

Combining Deep Learning Models We have introduced various deep learning models, which can be applied to different domains. For example, LSTM is mainly used for dealing with sequential data such as texts while the CNN is powerful for images. It is very common that we need to work on tasks which are related to different domains. In such cases, we can combine different deep learning models to propose a new framework that can be applied for the task at hand. For example, for an information retrieval task given a text query, we want to retrieve images that match the query. We will need to use LSTM or Word2Vec to learn a representation that captures the semantic meanings of the query. At the same time, we need to use CNN to learn features that describe the image. We can then train LSTM and CNN so that the similarity of the representations for the matched query-image pairs are maximized while the similarity of the representations for the non-matched query-image pairs are minimized. Another example is video action recognition, where we want to classify the action of the video. Since the video is composed of frames and nearby frames have dependency, a video is inherently sequential data and LSTM is a good fit for modeling such data. However, LSTM is not good at extracting images. Therefore, we will first need to use CNN to extract features from each frame of the video, which are then used as input to LSTM for learning representation of the video [68]. Similarly, for image captioning, we can use CNN to extract features and use LSTM to generate image captions based on the image features [71]. We just list a few examples and there are many other examples. In general, we can treat deep learning algorithms as feature extracting tools that can extract features from certain domains. We can then design a loss function on top of these deep learning algorithms for the problem we want to study. One thing to note is that when we combine different models together, they are trained end-to-end. In other words, we don't train these models separately. Instead, we treat the new model as a unified model. This usually gives better performance than training each model separately and then combining them.

Bibliography

[1] Ossama Abdel-Hamid, Abdel-Rahman Mohamed, Hui Jiang, Li Deng, Gerald Penn, and Dong Yu. Convolutional neural networks for speech recognition. *IEEE/ACM Transactions on Audio, Speech, and Language Processing*, 22(10):1533–1545, 2014.

[2] Stanislaw Antol, Aishwarya Agrawal, Jiasen Lu, Margaret Mitchell, Dhruv Batra, C. Lawrence Zitnick, and Devi Parikh. VQA: Visual question answering. In *CVPR*, pages 2425–2433, 2015.

[3] Sarath Chandar AP, Stanislas Lauly, Hugo Larochelle, Mitesh Khapra, Balaraman Ravindran, Vikas C Raykar, and Amrita Saha. An autoencoder approach to learning bilingual word representations. In *NIPS*, pages 1853–1861, 2014.

[4] Yoshua Bengio et al. Learning deep architectures for AI. *Foundations and Trends in Machine Learning*, 2(1):1–127, 2009.

[5] Samuel R Bowman, Luke Vilnis, Oriol Vinyals, Andrew M Dai, Rafal Jozefowicz, and Samy Bengio. Generating sentences from a continuous space. *CoNLL*, 2016.

[6] Xi Chen, Yan Duan, Rein Houthooft, John Schulman, Ilya Sutskever, and Pieter Abbeel. Infogan: Interpretable representation learning by information maximizing generative adversarial nets. In *NIPS*, pages 2172–2180, 2016.

[7] Kyunghyun Cho, Bart Van Merriënboer, Caglar Gulcehre, Dzmitry Bahdanau, Fethi Bougares, Holger Schwenk, and Yoshua Bengio. Learning phrase representations using RNN encoder-decoder for statistical machine translation. *arXiv preprint arXiv:1406.1078*, 2014.

[8] Aaron Courville, James Bergstra, and Yoshua Bengio. A spike and slab restricted boltzmann machine. In *AISTAS*, pages 233–241, 2011.

[9] George Dahl, Abdel-Rahman Mohamed, Geoffrey E Hinton, et al. Phone recognition with the mean-covariance restricted Boltzmann machine. In *NIPS*, pages 469–477, 2010.

[10] Michaël Defferrard, Xavier Bresson, and Pierre Vandergheynst. Convolutional neural networks on graphs with fast localized spectral filtering. In *NIPS*, pages 3844–3852, 2016.

[11] Emily Denton and Vighnesh Birodkar. Unsupervised learning of disentangled representations from video. pages 4417–4426, NIPS 2017.

[12] Clement Farabet, Camille Couprie, Laurent Najman, and Yann LeCun. Learning hierarchical features for scene labeling. *IEEE TPAMI*, 35(8):1915–1929, 2013.

[13] John R Firth. *A Synopsis of Linguistic Theory*, 1930-1955. 1957.

[14] Ross Girshick, Jeff Donahue, Trevor Darrell, and Jitendra Malik. Rich feature hierarchies for accurate object detection and semantic segmentation. In *CVPR*, pages 580–587, 2014.

[15] Ian Goodfellow, Yoshua Bengio, and Aaron Courville. *Deep Learning*. MIT Press, 2016.

[16] Ian Goodfellow, Jean Pouget-Abadie, Mehdi Mirza, Bing Xu, David Warde-Farley, Sherjil Ozair, Aaron Courville, and Yoshua Bengio. Generative adversarial nets. In *NIPS*, pages 2672–2680, 2014.

[17] Alex Graves, Abdel-Rahman Mohamed, and Geoffrey Hinton. Speech recognition with deep recurrent neural networks. In *ICASSP*, pages 6645–6649. IEEE, 2013.

[18] Karol Gregor, Ivo Danihelka, Alex Graves, Danilo Jimenez Rezende, and Daan Wierstra. Draw: A recurrent neural network for image generation. *arXiv preprint arXiv:1502.04623*, 2015.

[19] Kaiming He, Xiangyu Zhang, Shaoqing Ren, and Jian Sun. Deep residual learning for image recognition. In *CVPR*, pages 770–778, 2016.

[20] Geoffrey Hinton, Li Deng, Dong Yu, George E Dahl, Abdel-Rahman Mohamed, Navdeep Jaitly, Andrew Senior, Vincent Vanhoucke, Patrick Nguyen, Tara N Sainath, et al. Deep neural networks for acoustic modeling in speech recognition: The shared views of four research groups. *IEEE Signal Processing Magazine*, 29(6):82–97, 2012.

[21] Geoffrey E Hinton. Deep belief networks. *Scholarpedia*, 4(5):5947, 2009.

[22] Geoffrey E Hinton et al. Modeling pixel means and covariances using factorized third-order Boltzmann machines. In *CVPR*, pages 2551–2558. IEEE, 2010.

[23] Sepp Hochreiter and Jürgen Schmidhuber. Long short-term memory. *Neural Computation*, 9(8):1735–1780, 1997.

[24] Wei-Ning Hsu, Yu Zhang, and James R. Glass. Learning latent representations for speech generation and transformation. Annual Conference of the International Speech Communication Association, (INTERSPEECH). pages 1273–1277, 2017.

[25] Wei-Ning Hsu, Yu Zhang, and James R. Glass. Unsupervised learning of disentangled and interpretable representations from sequential data. In *NIPS*, 2017.

[26] Zhiting Hu, Zichao Yang, Xiaodan Liang, Ruslan Salakhutdinov, and Eric P Xing. Toward controllable text generation. In *ICML*, 2017.

[27] Ozan Irsoy and Claire Cardie. Opinion mining with deep recurrent neural networks. In *EMNLP*, pages 720–728, 2014.

[28] Michael Janner, Jiajun Wu, Tejas Kulkarn, Ilker Yildirim, and Josh Tenenbaum. Learning to generalize intrinsic images with a structured disentangling autoencoder. In *NIPS*, 2017.

[29] Nal Kalchbrenner, Edward Grefenstette, and Phil Blunsom. A convolutional neural network for modelling sentences. In *ACL*, 2014.

[30] Diederik P Kingma and Max Welling. Auto-encoding variational Bayes. *arXiv preprint arXiv:1312.6114*, 2013.

[31] Alex Krizhevsky, Geoffrey E Hinton, et al. Factored 3-way restricted Boltzmann machines for modeling natural images. In *AISTATS*, pages 621–628, 2010.

[32] Alex Krizhevsky, Ilya Sutskever, and Geoffrey E Hinton. Imagenet classification with deep convolutional neural networks. In *NIPS*, pages 1097–1105, 2012.

[33] Honglak Lee, Roger Grosse, Rajesh Ranganath, and Andrew Y Ng. Unsupervised learning of hierarchical representations with convolutional deep belief networks. *Communications of the ACM*, 54(10):95–103, 2011.

[34] Omer Levy and Yoav Goldberg. Neural word embedding as implicit matrix factorization. In *NIPS*, pages 2177–2185, 2014.

[35] Yang Li, Quan Pan, Tao Yang, Suhang Wang, Jiliang Tang, and Erik Cambria. Learning word representations for sentiment analysis. *Cognitive Computation*, 2017.

[36] Jonathan Long, Evan Shelhamer, and Trevor Darrell. Fully convolutional networks for semantic segmentation. In *CVPR*, pages 3431–3440, 2015.

[37] Jonathan Masci, Ueli Meier, Dan Cireşan, and Jürgen Schmidhuber. Stacked convolutional auto-encoders for hierarchical feature extraction. *Artificial Neural Networks and Machine Learning–ICANN 2011*, pages 52–59, 2011.

[38] Michaël Mathieu, Junbo Jake Zhao, Pablo Sprechmann, Aditya Ramesh, and Yann LeCun. Disentangling factors of variation in deep representation using adversarial training. In *NIPS*, pages 5041–5049, 2016.

[39] Tomas Mikolov, Kai Chen, Greg Corrado, and Jeffrey Dean. Efficient estimation of word representations in vector space. *arXiv preprint arXiv:1301.3781*, 2013.

[40] Tomas Mikolov, Martin Karafiát, Lukás Burget, Jan Cernocký, and Sanjeev Khudanpur. Recurrent neural network based language model. In *INTERSPEECH*, pages 1045–1048, 2010.

[41] Tomas Mikolov, Ilya Sutskever, Kai Chen, Greg S Corrado, and Jeff Dean. Distributed representations of words and phrases and their compositionality. In *NIPS*, pages 3111–3119, 2013.

[42] Abdel-Rahman Mohamed, George Dahl, and Geoffrey Hinton. Deep belief networks for phone recognition. In *NIPS Workshop on Deep Learning for Speech Recognition and Related Applications*, 2009.

[43] Andrew Ng. Sparse autoencoder. *CS294A Lecture Notes*, 72(2011):1–19, 2011.

[44] Jiquan Ngiam, Aditya Khosla, Mingyu Kim, Juhan Nam, Honglak Lee, and Andrew Y Ng. Multimodal deep learning. In *ICML*, pages 689–696, 2011.

[45] Maxime Oquab, Leon Bottou, Ivan Laptev, and Josef Sivic. Learning and transferring mid-level image representations using convolutional neural networks. In *CVPR*, pages 1717–1724, 2014.

[46] Jeffrey Pennington, Richard Socher, and Christopher D Manning. Glove: Global vectors for word representation. In *EMNLP*, volume 14, pages 1532–1543, 2014.

[47] Alec Radford, Luke Metz, and Soumith Chintala. Unsupervised representation learning with deep convolutional generative adversarial networks. *arXiv preprint arXiv:1511.06434*, 2015.

[48] Scott Reed, Kihyuk Sohn, Yuting Zhang, and Honglak Lee. Learning to disentangle factors of variation with manifold interaction. In *ICML*, pages 1431–1439, 2014.

[49] Salah Rifai, Yoshua Bengio, Aaron Courville, Pascal Vincent, and Mehdi Mirza. Disentangling factors of variation for facial expression recognition. *ECCV*, pages 808–822, 2012.

[50] Haşim Sak, Andrew Senior, and Françoise Beaufays. Long short-term memory recurrent neural network architectures for large scale acoustic modeling. In *Fifteenth Annual Conference of the International Speech Communication Association*, 2014.

[51] Ruslan Salakhutdinov and Geoffrey Hinton. Deep Boltzmann machines. In *Artificial Intelligence and Statistics*, pages 448–455, 2009.

[52] Ruhi Sarikaya, Geoffrey E. Hinton, and Anoop Deoras. Application of deep belief networks for natural language understanding. *IEEE/ACM Trans. Audio, Speech & Language Processing*, 22(4):778–784, 2014.

[53] Ali Sharif Razavian, Hossein Azizpour, Josephine Sullivan, and Stefan Carlsson. CNN features off-the-shelf: an astounding baseline for recognition. In *CVPR Workshops*, pages 806–813, 2014.

[54] N. Siddharth, Brooks Paige, Jan-Willem van de Meent, Alban Desmaison, Frank Wood, Noah D. Goodman, Pushmeet Kohli, and Philip H. S. Torr. Learning disentangled representations with semi-supervised deep generative models. In *NIPS*, 2017.

[55] Karen Simonyan and Andrew Zisserman. Two-stream convolutional networks for action recognition in videos. In *NIPS*, pages 568–576, 2014.

[56] Nitish Srivastava, Geoffrey E Hinton, Alex Krizhevsky, Ilya Sutskever, and Ruslan Salakhutdinov. Dropout: A simple way to prevent neural networks from overfitting. *Journal of Machine Learning Research*, 15(1):1929–1958, 2014.

[57] Nitish Srivastava and Ruslan R Salakhutdinov. Multimodal learning with deep Boltzmann machines. In *NIPS*, pages 2222–2230, 2012.

[58] Nitish Srivastava, Ruslan R Salakhutdinov, and Geoffrey E Hinton. Modeling documents with deep Boltzmann machines. In *UAI*, 2013.

[59] Heung-Il Suk, Seong-Whan Lee, Dinggang Shen, Alzheimer's Disease Neuroimaging Initiative, et al. Hierarchical feature representation and multimodal fusion with deep learning for AD/MCI diagnosis. *NeuroImage*, 101:569–582, 2014.

[60] Ilya Sutskever, Oriol Vinyals, and Quoc V Le. Sequence to sequence learning with neural networks. In *NIPS*, pages 3104–3112, 2014.

[61] Jian Tang, Meng Qu, Mingzhe Wang, Ming Zhang, Jun Yan, and Qiaozhu Mei. Line: Large-scale information network embedding. In *WWW*, pages 1067–1077, 2015.

[62] Tijmen Tieleman. Training restricted Boltzmann machines using approximations to the likelihood gradient. In *ICML*, pages 1064–1071. ACM, 2008.

[63] Pascal Vincent, Hugo Larochelle, Isabelle Lajoie, Yoshua Bengio, and Pierre-Antoine Manzagol. Stacked denoising autoencoders: Learning useful representations in a deep network with a local denoising criterion. *Journal of Machine Learning Research*, 11(Dec):3371–3408, 2010.

[64] Daixin Wang, Peng Cui, and Wenwu Zhu. Structural deep network embedding. In *SIGKDD*, pages 1225–1234. ACM, 2016.

[65] Jun Wang, Lantao Yu, Weinan Zhang, Yu Gong, Yinghui Xu, Benyou Wang, Peng Zhang, and Dell Zhang. Irgan: A minimax game for unifying generative and discriminative information retrieval models. In *SIGIR*, 2017.

[66] Suhang Wang, Jiliang Tang, Charu Aggarwal, and Huan Liu. Linked document embedding for classification. In *CIKM*, pages 115–124. ACM, 2016.

[67] Suhang Wang, Jiliang Tang, Fred Morstatter, and Huan Liu. Paired restricted Boltzmann machine for linked data. In *CIKM*, pages 1753–1762. ACM, 2016.

[68] Yilin Wang, Suhang Wang, Jiliang Tang, Neil O'Hare, Yi Chang, and Baoxin Li. Hierarchical attention network for action recognition in videos. *CoRR*, abs/1607.06416, 2016.

[69] Max Welling, Michal Rosen-Zvi, and Geoffrey E Hinton. Exponential family harmoniums with an application to information retrieval. In *NIPS*, volume 4, pages 1481–1488, 2004.

[70] Paul J Werbos. Backpropagation through time: What it does and how to do it. *Proceedings of the IEEE*, 78(10):1550–1560, 1990.

[71] Kelvin Xu, Jimmy Ba, Ryan Kiros, Kyunghyun Cho, Aaron Courville, Ruslan Salakhudinov, Rich Zemel, and Yoshua Bengio. Show, attend and tell: Neural image caption generation with visual attention. In *ICML*, pages 2048–2057, 2015.

[72] Xinchen Yan, Jimei Yang, Kihyuk Sohn, and Honglak Lee. Attribute2image: Conditional image generation from visual attributes. In *ECCV*, pages 776–791. Springer, 2016.

[73] Zichao Yang, Diyi Yang, Chris Dyer, Xiaodong He, Alexander J Smola, and Eduard H Hovy. Hierarchical attention networks for document classification. In *HLT-NAACL*, pages 1480–1489, 2016.

[74] Lantao Yu, Weinan Zhang, Jun Wang, and Yong Yu. Seqgan: Sequence generative adversarial nets with policy gradient. In *AAAI*, pages 2852–2858, 2017.

[75] Shengjia Zhao, Jiaming Song, and Stefano Ermon. Learning hierarchical features from deep generative models. In *ICML*, pages 4091–4099, 2017.

CHAPTER 6

NEURAL NETWORKS AND DEEP LEARNING

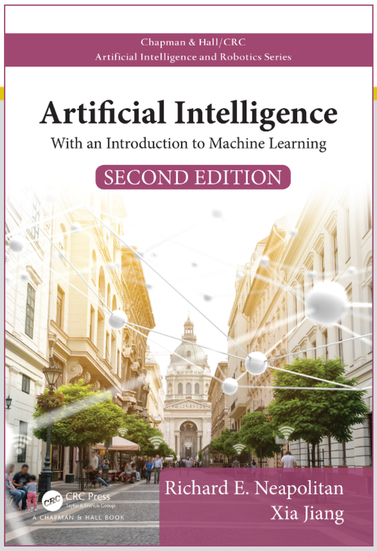

Neural Networks and Deep Learning

The previous three parts modeled intelligence at either a human cognitive level or at a population-based level. The intelligence is removed from the physiological processes involved in intelligent reasoning. In this part, we model the neuronal processes involved when the brain is "intelligently" controlling the thoughts and behavior of a life form. The networks we construct in this fashion are called **artificial neural networks**. Neural networks have been used effectively in applications such as image recognition and speech recognition, which are hard to model with the structured approach used in rule-based systems and Bayesian networks. In the case of image recognition, for example, they learn to identify images of cars by being presented with images that have been labeled "car" and "no car". We start by modeling a single neuron.

15.1 The Perceptron

Figure 15.1 (a) shows a biological neuron, which has dendrites that transmit signals to a cell body, a cell body that processes the signal, and an axon that sends signals out to other

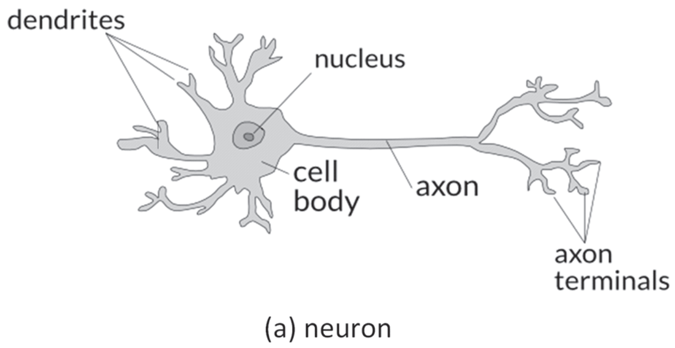

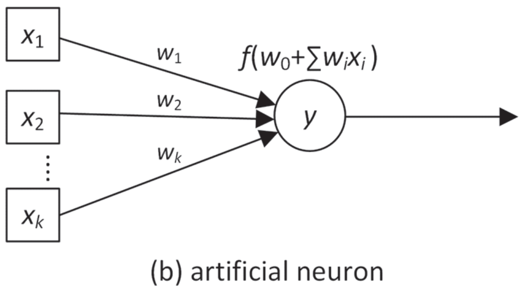

Figure 15.1 A neuron is in (a); an artficial neuron is in (b).

neurons. The input signals are accumulated in the cell body of the neuron, and if the accumulated signal exceeds a certain threshold, an output signal is generated which is passed on by the axon. Figure 15.1 (b) show an artificial neuron that mimics this process. The artificial neuron takes as input a vector $(x_1, x_2, ..., x_k)$, and then applies **weights** $(w_0, w_1, w_2, ..., w_k)$ to that input yielding a weighted sum:

$$w_0 + \sum_{i=1}^{k} w_i x_i.$$

Next the neuron applies an activation function f to that sum, and outputs the value y of f. Note that the inputs x_i are square nodes to distinguish them from an artificial neuron, which is a computational unit.

A **neural network** consists of one to many artificial neurons, which communicate with each other. The output of one neuron is the input to another neuron. The simplest neural network is the **perceptron**, which consists of a single artificial neuron, as shown in Figure 15.1 (b). The activation function for the perceptron is as follows:

$$f(z) = \begin{cases} 1 & \text{if } z > 0 \\ -1 & \text{otherwise} \end{cases}$$

Therefore, the complete expression for the output y of the perceptron is as follows:

$$y = \begin{cases} 1 & \text{if } w_0 + \sum_{i=1}^{k} w_i x_i > 0 \\ -1 & \text{otherwise} \end{cases} \tag{15.1}$$

The perceptron is a binary classifier. It returns 1 if the activation function exceeds 0; otherwise it returns -1.

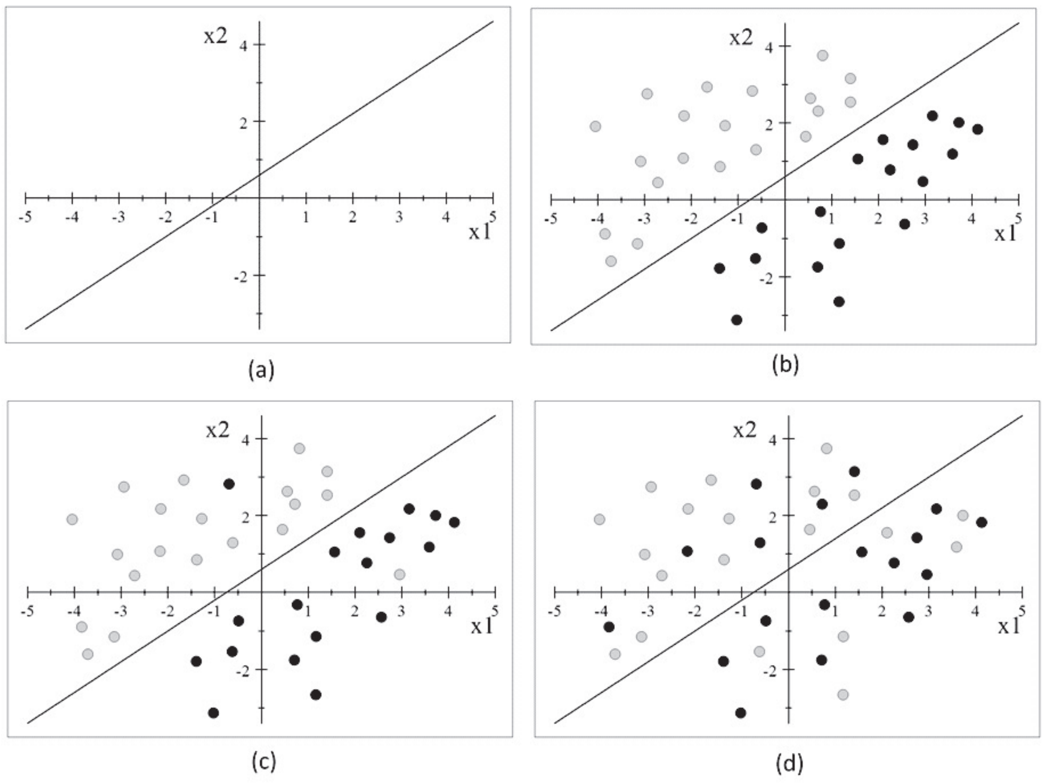

Figure 15.2 The line $-3 - 4x_1 + 5x_2 = 0$ is in (a). This line linearly separates the data in (b), and approximately linearly separates the data in (c). It does not approximately linearly separate the data in (d).

Let's look at the case where the input is a two-dimensional vector (x_1, x_2). Suppose the weighted sum in our perceptron is as follows:

$$w_0 + w_1x_1 + w_2x_2 = -3 - 4x_1 + 5x_2. \tag{15.2}$$

Figure 15.2 (a) plots the line $-3 - 4x_1 + 5x_2 = 0$. If we color 2-dimensional points gray or black, the set of gray points is **linearly separable** from the set of black points if there exists at least one line in the plane with all the gray points on one side of the line and all the black points on the other side. This definition extends readily to higher-dimensional data. The points in Figure 15.2 (b) are linearly separable by the line $-3 - 4x_1 + 5x_2 = 0$. So, the perceptron with the weights in Equality 15.2 maps all the gray points to $y = 1$, and all the black points to $y = -1$. This perceptron is a perfect binary classifier for these data. If we have the data in Figure 15.2 (c), this perceptron is a pretty good classifier, as it only misclassifies two cases. It is a very poor classifier for the data in Figure 15.2 (d). The gray and black points in that figure are not approximately linearly separable; so no perceptron would be a good classifier for this data. The perceptron is a **linear binary classifier** because it uses a linear function to classify an instance.

15.1.1 Learning the Weights for a Perceptron

When learning a perceptron for binary classification, our goal is to determine weights determining a line that as close as possible linearly separates the two classes. Next we develop a gradient descent algorithm for learning these weights (See Section 5.3.2 for an introduction to gradient descent.) If we have a data item $(x_1, x_2, ..., x_k, y)$, our loss function is

$$Loss(y, \hat{y}) = (\hat{y} - y)(w_0 + \sum_{i=1}^{k} w_i x_i),$$

where $\hat{y}$ is the estimate of y using Equation 15.1. The idea behind this loss function is that if $\hat{y} = y$ there is no loss. If $\hat{y} = 1$ and $y = -1$, then $w_0 + \sum_{i=1}^{k} w_i x_i > 1$, and the loss is $2\left(w_0 + \sum_{i=1}^{k} w_i x_i\right)$. This loss is a measure of how far off we are from obtaining a value < 0, which would have given a correct answer. Similarly, if $\hat{y} = -1$ and $y = 1$, then $w_0 + \sum_{i=1}^{k} w_i x_i < 1$, and the loss is again $2\left(w_0 + \sum_{i=1}^{k} w_i x_i\right)$. The cost function follows:

$$Cost([y^1, \hat{y}^1], ..., [y^n, \hat{y}^n]) = \sum_{j=1}^{n} Loss(y^j, \hat{y}^j) = \sum_{j=1}^{n} \left((\hat{y}^j - y^j)(w_0 + \sum_{i=1}^{k} w_i x_i^j) \right). \quad (15.3)$$

Note that x_i^j denotes the ith vector element in the jth data item. This is different from the notation used in Section 5.3. The partial derivatives of the cost function are as follows:

$$\frac{\partial \left(\sum_{j=1}^{n} (\hat{y}^j - y^j)(w_0 + \sum_{i=1}^{k} w_i x_i^j) \right)}{\partial w_0} = \sum_{j=1}^{n} (\hat{y}^j - y^j)$$

$$\frac{\partial \sum_{j=1}^{n} \left((\hat{y}^j - y^j)(w_0 + \sum_{i=1}^{k} w_i x_i^j) \right)}{\partial w_m} = \sum_{j=1}^{n} (\hat{y}^j - y^j) x_m^j.$$

When Rosenblatt [1958] developed the perceptron and the algorithm we are presenting, he updated based on each item in sequence as in stochastic gradient descent (Section 5.3.4). We show that version of the algorithm next.

Algorithm 15.1 Gradient_Descent_Perceptron

Input: Set of real predictor data and binary outcome data: $\{(x_1^1 x_2^1, ...x_k^1, y^1), (x_1^2 x_2^2, ...x_k^2, y^2)..., (x_1^n x_2^n, ...x_k^n, y^n)\}$.

Output: Weights $w_0, w_1, ..., w_k$ that minimize the cost function in Equality 15.3.

```
Function $Minimizing\_Values$;
for $i = 0$ to $k$
    $w_i = arbitrary\_value$;
endfor
$\lambda = learning\_rate$;
repeat $number\_iterations$ times
    for $j = 1$ to $n$
        $y = \left\{ \begin{array}{c} 1 \text{ if } w_0 + \sum_{i=1}^{k} w_i x_i^j > 0 \\ -1 \text{ otherwise} \end{array} \right.$
        $w_0 = w_0 - \lambda(y - y^j)$;
        for $m = 1$ to $k$
            $w_m = w_m - \lambda(y - y^j) x_m^j$;
        endfor
    endfor
endrepeat
```

Example 15.1 Suppose we set $\lambda = 0, 1$, and we have the following data:

x_1	x_2	y
1	2	1
3	4	-1

The algorithm through 2 iterations of the repeat loop follows:

// Initialize weights to arbitrary values.
$w_0 = 1; w_1 = 1, w_2 = 1;$

// First iteration of repeat loop.

// $j = 1$ in the for$-j$ loop.
$w_0 + w_1 x_1^1 + w_2 x_2^1 = 1 + 1(1) + 1(2) = 4 > 0;$
$y = 1;$
$w_0 = w_0 - \lambda(y - y^1) = 1 - (0.1)(1 - 1) = 1;$
$w_1 = w_1 - \lambda(y - y^1)x_1^1 = 1 - (0.1)(1 - 1)1 = 1;$
$w_2 = w_2 - \lambda(y - y^1)x_2^1 = 1 - (0.1)(1 - 1)2 = 1;$

// $j = 2$ in the for$-j$ loop.
$w_0 + w_1 x_1^2 + w_2 x_2^2 = 1 + 1(3) + 1(4) = 8 > 0;$
$y = 1;$
$w_0 = w_0 - \lambda(y - y^1) = 1 - (0.1)(1 - (-1)) = 0.8;$
$w_1 = w_1 - \lambda(y - y^1)x_1^1 = 1 - (0.1)(1 - (-1))3 = 0.4;$
$w_2 = w_2 - \lambda(y - y^1)x_2^1 = 1 - (0.1)(1 - (-1))4 = 0.2;$

// Second iteration of repeat loop.

// $j = 1$ in the for$-j$ loop.
$w_0 + w_1 x_1^1 + w_2 x_2^1 = 0.8 + 0.4(1) + 0.2(2) = 1.6 > 0;$
$y = 1;$
$w_0 = w_0 - \lambda(y - y^1) = 0.8 - (0.1)(1 - 1) = 0.8;$
$w_1 = w_1 - \lambda(y - y^1)x_1^1 = 0.4 - (0.1)(1 - 1)1 = 0.4;$
$w_2 = w_2 - \lambda(y - y^1)x_2^1 = 0.2 - (0.1)(1 - 1)2 = 0.2;$

// $j = 2$ in the for$-j$ loop.
$w_0 + w_1 x_1^2 + w_2 x_2^2 = 0.8 + 0.4(3) + 0.2(4) = 2.8 > 0;$
$y = 1;$
$w_0 = w_0 - \lambda(y - y^1) = 0.8 - (0.1)(1 - (-1)) = 0.6;$
$w_1 = w_1 - \lambda(y - y^1)x_1^1 = 0.4 - (0.1)(1 - (-1))3 = -0.2;$
$w_2 = w_2 - \lambda(y - y^1)x_2^1 = 0.2 - (0.1)(1 - (-1))4 = -0.6;$

Table 15.1 SAT Scores, Parental Income, and Graduation Status for 12 Students

SAT (100)	Income ($10,000)	Graduate
4	18	no
6	7	no
8	4	no
10	6	no
12	2	no
10	10	no
6	6	yes
7	20	yes
8	16	yes
12	16	yes
14	7	yes
16	4	yes

15.1.2 The Perceptron and Logistic Regression

The perceptron is similar to logistic regression (See Section 5.3.3) in that they both map continuous predictors to a binary outcome. The difference is that the perceptron deterministically reports that $Y = 1$ or $Y = -1$, while logistic regression reports the probability that $Y = 1$. Recall this logistic regression computes this probability as follows:

$$\begin{aligned} P(Y=1|\mathbf{x}) &= \frac{\exp(b_0 + \sum_{i=1}^k b_i x_i)}{1+\exp(b_0 + \sum_{i=1}^k b_i x_i)} \\ P(Y=-1|\mathbf{x}) &= \frac{1}{1+\exp(\sum_{i=1}^k b_i x_i)}. \end{aligned}$$

We can use the logistic regression equation as a binary classifier if we say $Y = 1$ if and only if $P(Y = 1) > P(Y = -1)$. The following sequence of steps shows that if we do this, we have a linear binary classifier.

$$\begin{aligned} P(Y=1|x) &= P(Y=-1|\mathbf{x}) \\ \frac{\exp(b_0 + \sum_{i=1}^k b_i x_i)}{1+\exp(b_0 + \sum_{i=1}^k b_i x_i)} &= \frac{1}{1+\exp(\sum_{i=1}^k b_i x_i)} \\ \exp\left(b_0 + \sum_{i=1}^k b_i x_i\right) &= 1 \\ \ln\left(\exp(b_0 + \sum_{i=1}^k b_i x_i)\right) &= 0 \\ b_0 + \sum_{i=1}^k b_i x_i &= 0. \end{aligned}$$

So, we set $Y = 1$ if and only if $b_0 + \sum_{i=1}^k b_i x_i > 0$.

Example 15.2 Suppose we suspect that SAT scores and parental income have an affect on whether a student graduates college, and we obtain the data in Table 15.1. These data are plotted in Figure 15.3 (a). If we learn a logistic regression model from these data (using an algorithm such as the one outlined in Section 5.3.3), we obtain

$$P(Graduate = yes|SAT, Income) = \frac{\exp(-6.24 + 0.439SAT + 0.222Income)}{1+\exp(-6.24 + 0.439SAT + 0.222Income)},$$

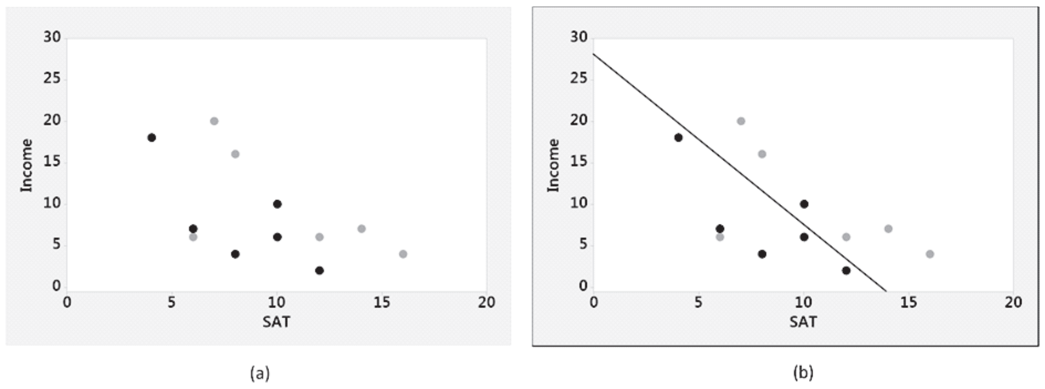

Figure 15.3 The plot in (a) shows individuals who graduated college as gray points and individuals who did not graduate college as black points. The plot in (b) shows the same individuals and includes the line $6.14 + 0.439SAT + 0.222Income$.

and so the line we obtain for a linear classifier is

$$-6.24 + 0.439SAT + 0.222Income = 0.$$

That line is plotted with the data in Figure 15.3 (b). Note that the line does not perfectly linearly separate the data, and two points are misclassified. These data are not linearly separable.

It is left as an exercise to implement Algorithm 15.1, apply it to the data in Table 15.1, and compare the results to those obtained with logistic regression.

15.2 Feedforward Neural Networks

If we want to classify the objects in Figure 15.2 (d), we need to go beyond a simple perceptron. Next we introduce more complex networks, which can classify objects that are not linearly separable. We start with a simple example, the XOR function.

15.2.1 Modeling XOR

The domain of the XOR function is $\{(0,0),(0,1)(1,0),(1,1)\}$. The XOR mapping is then as follows:

$$\begin{aligned}
XOR(0,0) &= 0 \\
XOR(0,1) &= 1 \\
XOR(1,0) &= 1 \\
XOR(1,1) &= 0.
\end{aligned}$$

Figure 15.4 plots the domain of the XOR function, and shows points mapping to 0 as black points and points mapping to 1 as gray points. Clearly, the black and gray points are not linearly separable. So, no perceptron could model the XOR function. However, the more complex network in Figure 15.5 does model it. That network is a **2-layer neural network** because there are two layers of artificial neurons. The first layer, containing the nodes h_1 and h_2, is called a hidden layer because it represents neither input nor output. The second layer contains the single output node y. The perceptron only has this layer. Note

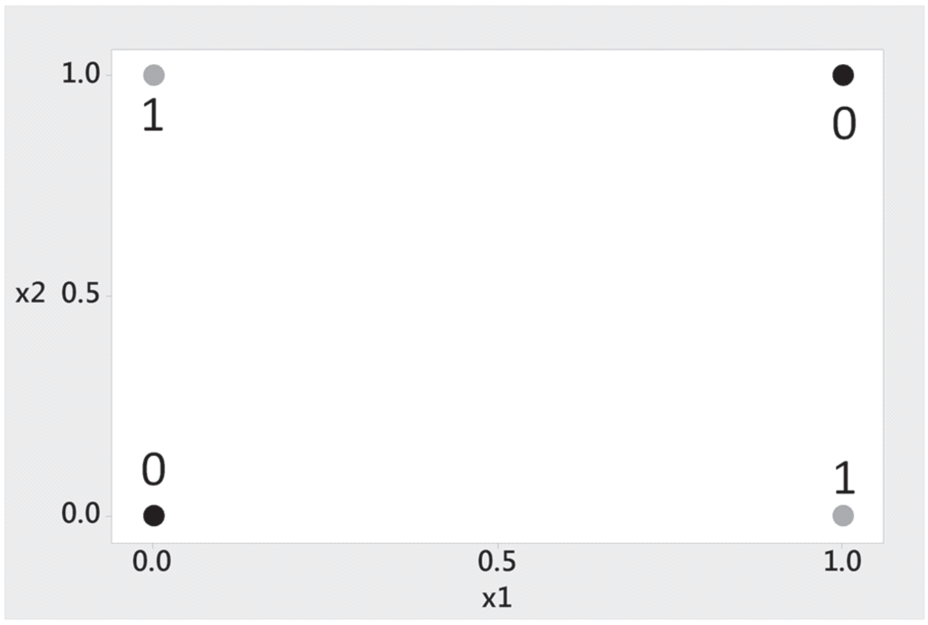

Figure 15.4 The XOR function. The black points map to 0, and the gray points map to 1.

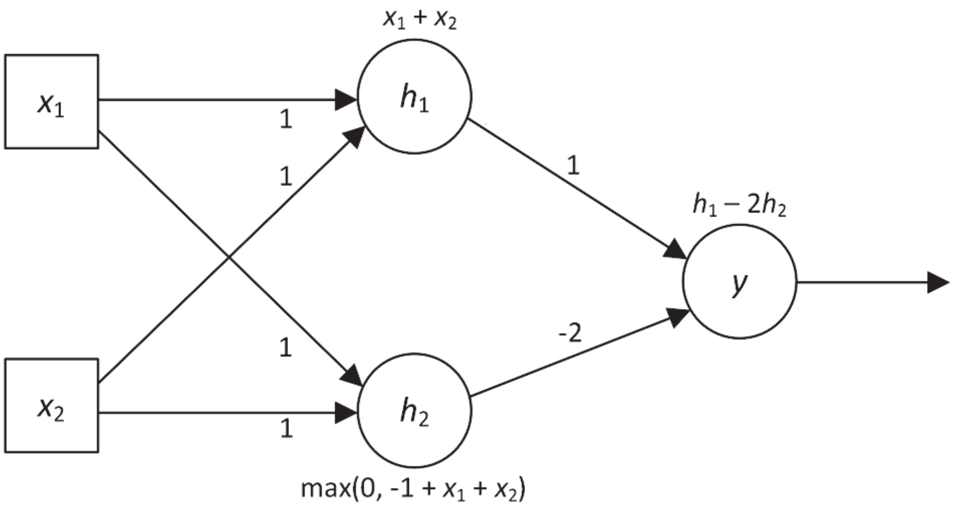

Figure 15.5 A neural network modeling the XOR function.

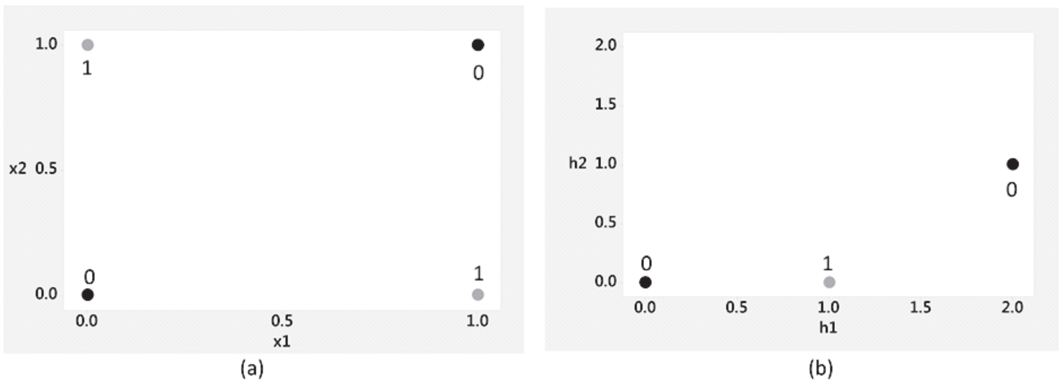

Figure 15.6 The original x-space is in (a), and the transformed h-space is in (b).

that the activation function in the hidden node h_2 in Figure 15.5 is $\max(0, z)$; this function is called the **rectified linear activation function**.

Let's show that the network in Figure 15.5 does indeed model the XOR function:

$$\begin{aligned}(x_1, x_2) &= (0,0)\\ h_1 &= 0+0=0\\ h_2 &= \max(0,-1+0+0)=0\\ y &= 0-2(0)=0\end{aligned}$$

$$\begin{aligned}(x_1, x_2) &= (0,1)\\ h_1 &= 0+1=1\\ h_2 &= \max(0,-1+0+1)=0\\ y &= 1-2(0)=1\end{aligned}$$

$$\begin{aligned}(x_1, x_2) &= (1,0)\\ h_1 &= 1+0=1\\ h_2 &= \max(0,-1+1+0)=0\\ y &= 1-2(0)=1\end{aligned}$$

$$\begin{aligned}(x_1, x_2) &= (1,1)\\ h_1 &= 1+1=2\\ h_2 &= \max(0,-1+1+1)=1\\ y &= 2-2(1)=0.\end{aligned}$$

The "trick" in this network is that h_1 and h_2 together map (0,0) to (0,0), (0,1) to (1,0), (1,0) to (1,0) and (1,1) to (2,1). So our black points are now (0,0) and (2,1), while our single gray point is (1,0). The data is now linearly separable. Figure 15.6 shows the transformation from the x-space to the h-space.

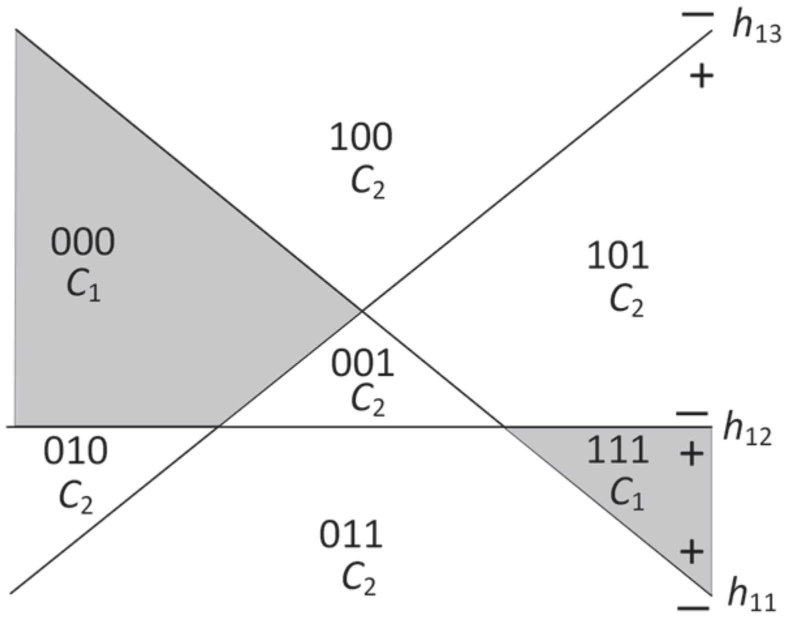

Figure 15.7 Class C_1 consists of the shaded area, and class C_2 consists of the white area. The notation 100, for example, means that the region lies on the plus side of line h_{11}, on the minus side of line h_{12}, and on the minus side of line h_{13}.

15.2.2 Example with Two Hidden Layers

Suppose we are classifying points in the plane, and all points in the grey area in Figure 15.7 are in class C_1, while all points in the white area are in class C_2. This is a difficult classification problem because the regions that comprise class C_1 are not even adjacent. The neural network in Figure 15.8, which has two hidden layers, correctly accomplishes this classification with appropriate weights and activation functions. Next, we show how this is done.

The lines h_1, h_2, and h_3 in Figure 15.7 separate the plane into 7 regions. The notation $+/-$ in Figure 15.7 indicates the region is on the + side of the given line or on the − side. We assign the region value 1 if it is on the + side of the line and value 0 if it is on the − side. Region 100 is therefore labeled as such because it is on the + side of line h_{11}, on the − side of line h_{12}, and on the − side of line h_{13}. The other regions are labeled in a similar fashion. We can create a hidden node h_{11} with weights representing line h_{11}. Then we use an activation function that returns 0 if (x_1, x_2) is on the − side of line h_{11} and 1 otherwise. We create hidden nodes h_{12} and h_{13} in a similar fashion. Table 15.2 shows the values output by each of the nodes h_{11}, h_{12}, and h_{13} when (x_1, x_2) resides in each of the 7 regions in Figure 15.7 (note that 110 does not determine a region). So, the regions map to the 7 of the corners of the unit cube in 3-space. The two points that represent class C_1 are (0,0,0) and (1,1,1). We can linearly separate point 0,0,0) from the other 6 points with a plane in 3-space. So we create a hidden node h_{21} that does this. We use an activation function that returns 1 for point (0,0,0) and 0 for all other points on the cube. Similarly, we create a hidden node h_{22} that outputs 1 for point (1,1,1) and 0 for all other points on the cube. Table 15.2 shows these values. So, the output of these two hidden nodes is (1,0)

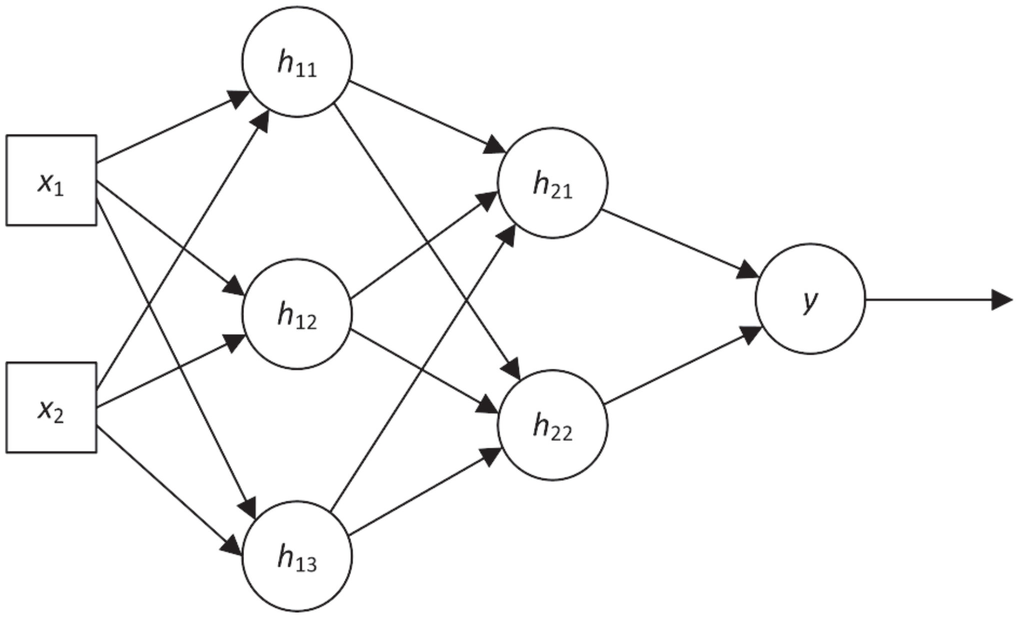

Figure 15.8 A neural network that correctly classifies points in classes C_1 and C_2 in Figure 15.7.

Table 15.2 Values of the Nodes in the Neural Network in Figure 15.7 for the Input Tuple Located in Each of the Regions in Figure 15.6

Region	Class	h_{11}	h_{12}	h_{13}	h_{21}	h_{22}	y
000	C_1	0	0	0	1	0	1
001	C_2	0	0	1	0	0	0
010	C_2	0	1	0	0	0	0
011	C_2	0	1	1	0	0	0
100	C_2	1	0	0	0	0	0
101	C_2	1	0	1	0	0	0
110	–	–	–	–	–	–	–
111	C_1	1	1	1	0	1	1

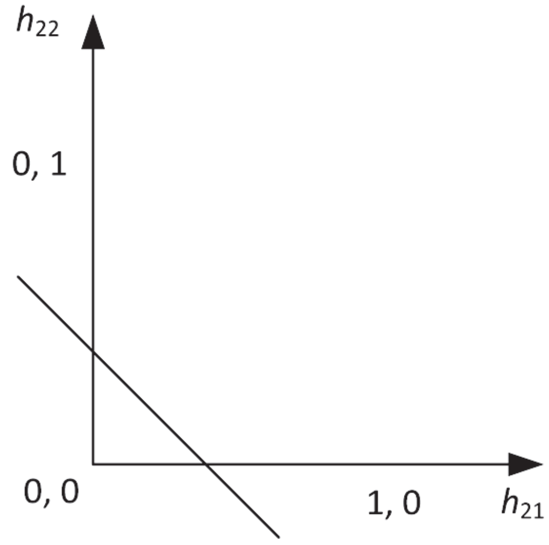

Figure 15.9 The points in region 000 map to (0,1), the points in region 111 map to (1,0), and all other points map to 0,0).

if (x_1, x_2) is in region 000 and (0,1) if (x_1, x_2) is in region 111. It is (0,0) if (x_1, x_2) is in any other region. These three points are shown in Figure 15.9. Next, we create weights for our output node y that yield a line that separates (1,0) and (0,1) from (0,0). Such a line is shown in Figure 15.9. We then use an activation function that returns 1 if the point lies above that line and 0 otherwise. In this way, all values of (x_1, x_2) in class C_1 map to 1 and all values of (x_1, x_2) in class C_2 map to 0.

Example 15.3 Suppose the three lines determining the regions in Figure 15.7 are as follows:

$$\begin{aligned} h_{11} &: \quad 2 - x_1 - x_2 = 0 \\ h_{12} &: \quad 0.5 - x_2 = 0 \\ h_{13} &: \quad x_1 - x_2 = 0. \end{aligned}$$

These three lines are plotted in Figure 15.10. Given these lines, the activation functions for hidden nodes h_{11}, h_{12}, and h_{13} are as follows:

$$h_{11} = \begin{cases} 1 & \text{if } 2 - x_1 - x_2 > 0 \\ 0 & \text{otherwise} \end{cases}$$

$$h_{12} = \begin{cases} 1 & \text{if } 0.5 - x_2 < 0 \\ 0 & \text{otherwise} \end{cases}$$

$$h_{12} = \begin{cases} 1 & \text{if } x_1 - x_2 < 0 \\ 0 & \text{otherwise} \end{cases} .$$

Hidden node h_{21} must provide a plane that linearly separates $(0,0,0)$ from all other points on the unit cube. The following is one such plane:

$$h_{11} + h_{12} + h_{13} = 0.5.$$

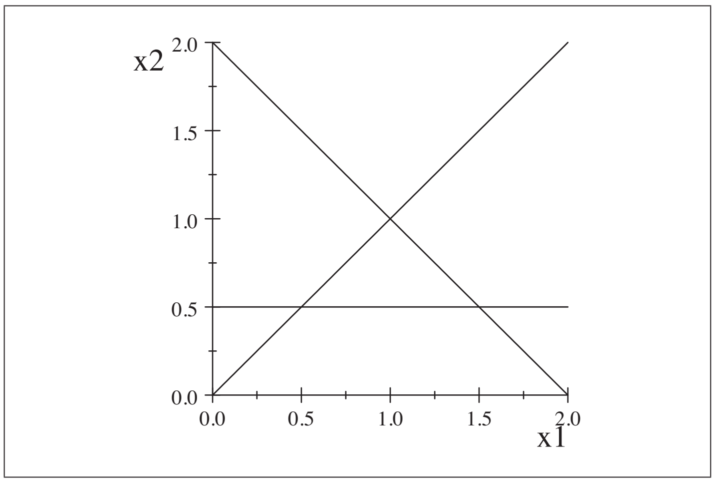

Figure 15.10 The three lines determining the regions in Figure 15.7 for Example 15.3.

So, we can make the activation function for hidden node h_{21} as follows:

$$h_{21} = \begin{cases} 1 & \text{if } h_{11} + h_{12} + h_{13} - 0.5 < 0 \\ 0 & \text{otherwise} \end{cases}$$

Hidden node h_{22} must provide a plane that linearly separates $(1, 1, 1)$ from all other points on the unit cube. The following is one such plane:

$$h_{11} + h_{12} + h_{13} = 2.5.$$

So, we can make the activation function for hidden node h_{22} as follows:

$$h_{22} = \begin{cases} 1 & \text{if } h_{11} + h_{12} + h_{13} - 2.5 > 0 \\ 0 & \text{otherwise} \end{cases} .$$

Finally node y must provide a line that linearly separates $(0, 1)$ and $(1, 0)$ from $(1, 1)$. The following is one such line:

$$h_{21} + h_{22} = 0.5.$$

So, we can make the activation function for node y as follows:

$$y = \begin{cases} 1 & \text{if } h_{21} + h_{22} - 0.5 > 0 \\ 0 & \text{otherwise} \end{cases} .$$

15.2.3 Structure of a Feedforward Neural Network

Having shown a neural network with one hidden layer (Figure 15.5) and a neural network with two hidden layers (Figure 15.8), we now present the general structure of a feedforward neural network. This structure appears in Figure 15.11. On the far left is the input, which consists of $x_1, x_2, ..., x_k$. Next there are 0 or more hidden layers. Then on the far right is the output layer, which consists of 1 or more nodes $y_1, y_2, ...y_m$. Each hidden layer can contain a different number of nodes.

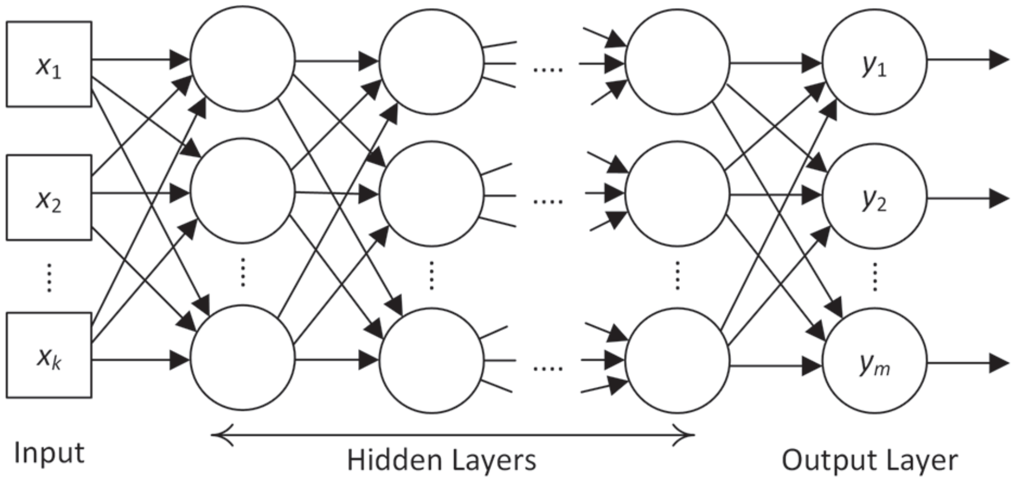

Figure 15.11 The general structure of a feedforward neural network.

In Sections 15.2.1 and 15.2.2 we constructed the neural network, and assigned values to the weights to achieve our desired results. Typically, we do not do this but rather learn the weights using a gradient descent algorithm similar to, but more complex than, the Algorithm 15.1 for the perceptron. For example, we could first construct the network in Figure 15.8 and then provide the form of the activation functions for the hidden nodes and the output node (discussed in the next section). Finally, we provide many data items to the algorithm, each of which has value $(x_1, x_2, ..., x_k, C)$, where C is the class to which point $(x_1, x_2, ..., x_k)$ belongs. The algorithm then learns weights such that the resultant network can classify new points.

A difficulty is that we don't know which network structure will work for a given problem beforehand. For example, without a detailed analysis of the problem in Section 15.2.2, we would not know to assign two hidden layers where the first layer contains 3 nodes, and the second layer contains 2 nodes. So, in general we experiment with different network configurations, and using a technique such as cross validation (Section 5.2.3), we find the configuration that gives the best results. There are various strategies for configuring the network. One strategy is to make the number of hidden nodes about equal to the number of input variables, and assign various layer and node per layer configurations. However, this will probably result in over-fitting if the dataset size is small compared to the input size. Another strategy is to make the number of hidden nodes no greater than the number of data items, and again try various layer and node per layer configurations.

In summary, to develop a neural network application we need data on the input variable(s) and output variable(s). We then construct a network with some configuration of hidden node layers and an output layer. The final step is to specify the activation functions, which we discuss next. Note that, if implementing the neural network from scratch, we would also need to program the gradient descent algorithm that finds the optimal values of the weights. However, henceforth we will assume that we are using a neural network package which has these algorithms implemented. We will present such packages in the final section.

15.3 Activation Functions

Next we discuss the activation functions that are ordinarily used in neural

networks.

15.3.1 Output Nodes

We have different activation functions for the output nodes depending on the task. If we are classifying data into one of two different classes, we need output nodes that represent binary classification. If we are classifying data in one of three or more possible classes, we need output nodes that represent multinomial classification. If our output is a continuous distribution such as the normal distribution, we need nodes that represent properties of that distribution. We discuss each in turn.

15.3.1.1 Binary Classification

In binary classification we want to classify or predict a variable that has two possible values. For example, we may want to predict whether a patient's cancer will metastasize based on features of the patient's cancer. In most such cases we do not want the system to simply say "yes" or "no". Rather we want to know, for example, the probability of the cancer metastasizing. So rather than using the discrete activation function that was used in the perceptron, we ordinarily use the **sigmoid function**, which is also used in logistic regression (Section 5.3.3). So, assuming the single output node y has the vector of hidden nodes $\mathbf{h}$ as parents, the **sigmoid activation function** for a binary outcome is

$$f(\mathbf{h}) = \frac{\exp(w_0 + \sum w_i h_i)}{1 + \exp(w_0 + \sum w_i h_i)}, \tag{15.4}$$

which yields $P(Y = 1|\mathbf{h})$.

Example 15.4 Suppose our output function is the sigmoid function, and

$$w_0 = 2, w_1 = -4, w_2 = -3, w_3 = 5.$$

Suppose further that for a particular input

$$h_1 = 6, h_2 = 7, h_3 = 9.$$

Then

$$\begin{aligned} f(\mathbf{h}) &= \frac{\exp(w_0 + w_1 \times h_1 + w_2 \times h_2 + w_3 \times h_3)}{1 + \exp(w_0 + w_1 \times h_1 + w_2 \times h_2 + w_3 \times h_3)} \\ &= \frac{\exp(2 - 4 \times 6 - 3 \times 7 + 5 \times 9)}{1 + \exp(2 - 4 \times 6 - 3 \times 7 + 5 \times 9)} \\ &= 0.881. \end{aligned}$$

So,

$$P(Y = 1|\mathbf{h}) = 0.881.$$